

Reproducibility in high-throughput density functional theory: a comparison of AFLOW, Materials Project, and OQMD

Vinay I. Hegde,^{1,*} Christopher K. H. Borg,^{1,*} Zachary del Rosario,^{1,2} Yoolhee Kim,¹ Maxwell Hutchinson,¹ Erin Antono,¹ Julia Ling,¹ Paul Saxe,³ James E. Saal,¹ and Bryce Meredig^{1,†}

¹Citrine Informatics, 2629 Broadway, Redwood City, CA 94063

²Olin College of Engineering, 1000 Olin Way, Needham, MA 02492

³Molecular Sciences Software Institute, Virginia Tech, Blacksburg, VA 24061

(Dated: July 7, 2020)

A central challenge in high throughput density functional theory (HT-DFT) calculations is selecting a combination of input parameters and post-processing techniques that can be used across all materials classes, while also managing accuracy-cost tradeoffs. To investigate the effects of these parameter choices, we consolidate three large HT-DFT databases: Automatic-FLOW (AFLOW), the Materials Project (MP), and the Open Quantum Materials Database (OQMD), and compare reported properties across each pair of databases for materials calculated using the same initial crystal structure. We find that HT-DFT formation energies and volumes are generally more reproducible than band gaps and total magnetizations; for instance, a notable fraction of records disagree on whether a material is metallic (up to 7%) or magnetic (up to 15%). The variance between calculated properties is as high as 0.105 eV/atom (median relative absolute difference, or MRAD, of 6%) for formation energy, 0.65 Å³/atom (MRAD of 4%) for volume, 0.21 eV (MRAD of 9%) for band gap, and 0.15 μ_B/formula unit (MRAD of 8%) for total magnetization, comparable to the differences between DFT and experiment. We trace some of the larger discrepancies to choices involving pseudopotentials, the DFT+*U* formalism, and elemental reference states, and argue that further standardization of HT-DFT would be beneficial to reproducibility.

Keywords: HT-DFT, MGI, reproducibility, uncertainty, informatics

I. INTRODUCTION

Over the past decade, high-throughput (HT) density functional theory (DFT) has emerged as a widely-used tool for materials discovery and design^{1–3}. In a standard HT-DFT workflow, software tools automate the process of calculating materials properties of interest within DFT, including submitting jobs to high-performance computing infrastructure, on-the-fly error handling, post-processing and dissemination of results, and so on, enabling researchers to evaluate typically 10³–10⁶ materials with minimal human intervention. The resulting database can then be screened for candidate materials exhibiting promising combinations of calculated properties or to search for trends amongst materials behavior to gain new physical insights or develop surrogate models.

The increasingly widespread usage of HT-DFT in materials research can be attributed to a combination of three key factors. First, a large number of specialized codes implement fully automated calculations of specific materials properties within DFT, ranging from phonon dispersions to dielectric tensors. For example, VASP 5.1^{4,5} introduced a feature enabling users to calculate elastic tensors by simply setting a parameter in the input file. Second, the ongoing growth of computing power has ensured that HT-DFT is now well within reach of a single university research group. Third, sophisticated, free, often open-source, software are readily available for managing large numbers of DFT calculations, post-processing output, and storing the resulting data systematically in

databases. Thus, a number of HT-DFT databases with various focus areas have emerged; a list of exemplars, including any supporting workflow automation software, is given in Section I of the Supplementary Information.

However, the entirely-automated nature of HT-DFT introduces a few key challenges. First, by definition, the volume of data from HT-DFT is too high for each individual calculation to undergo manual review or analysis¹. How, then, are the quality and integrity of calculations monitored in high-throughput? Second, HT-DFT requires choosing, often at the outset, settings that are consistent across all calculations, encompassing all materials classes and properties being calculated. For example, it may not be known *a priori* whether the material being calculated is a metal or an insulator. As a result, the calculation parameters that affect, e.g., how electronic occupancies are smeared near the Fermi level must be chosen so that they are applicable to both metals and insulators. Third, practical HT-DFT calculations involve balancing accuracy and computational cost; best-practice recommendations⁶ involve steps such as explicit convergence tests, which become computationally infeasible in the HT context.

Since HT-DFT has become increasingly central to materials informatics efforts across the spectrum, from high-throughput screening to machine learning^{7,8}, it is crucial to resolve the following concerns: (a) There is no one “correct” solution to some of the challenges of HT-DFT mentioned above, and different databases have tackled them slightly differently. How sensitive are the calculated materials properties to the different HT-DFT parameter choices? (b) The focus areas of many prominent HT-

DFT databases in terms of the materials and properties calculated are often quite different. How interoperable are these various calculated materials properties across HT-DFT databases? We emphasize that such a comparison across HT-DFT databases is different from analyzing the reproducibility of DFT across software implementations and potentials, e.g. focusing on equations of state of elemental crystals⁹: the challenges of HT-DFT lie in choosing parameters that are applicable across a wide variety of materials and properties, targeting both reasonable accuracy *and* computational cost—very distinct from performing highly-accurate DFT calculations of a small set of materials.

Here, we analyze the reproducibility and interoperability of HT-DFT calculations, and demonstrate the benefits of centralizing multiple HT-DFT databases onto a single platform. We critically compare the agreement between three databases for four properties: formation energy (ΔE_f), volume (V), band gap (E_g), and total magnetization (M). We find certain properties (formation energies and volumes) to be more consistent across databases than others (band gap and magnetization). We then quantify the variability in each of the properties across databases and find that the typical differences between two HT-DFT databases are similar to those between DFT and experiment. Finally, we compare properties across different materials classes to identify characteristics of materials and/or properties that are harder than others to reproduce. In all cases, we identify trends, surface outliers, and investigate potential causes for an observed systematic differences between the databases.

II. METHODS

We focus on three prominent HT-DFT databases in this work: Automatic FLOW (AFLOW)¹⁰, the Materials Project (MP)¹¹, and the Open Quantum Materials Database (OQMD)^{3,12}. All three databases contain calculations of a large number of mostly-experimentally reported, ordered compounds from the Inorganic Crystal Structure Database (ICSD)¹³. In addition, they contain calculations of many thousands of hypothetical compounds generated from common structural prototypes or other informatics approaches. We note here that all three databases use the VASP software package^{4,5} and projector augmented wave (PAW) potentials^{14,15} with the Perdew-Burke-Ernzerhof (PBE) parameterization¹⁶ of a generalized-gradient approximation (GGA) to the DFT exchange-correlation functional. The variance in HT-DFT-calculated properties studied in the present work is, therefore, almost entirely due to differences in various parameter choices involved in HT-DFT, and not due to different implementations of DFT or approximations to the exchange-correlation functional.

AFLOW has standardized band structure calculations¹⁷, binary alloy cluster expansions¹⁸, finite-temperature thermodynamic properties¹⁹ calculated for

many materials, and has an application programming interface (API) for accessing data²⁰. The Materials Project includes a variety of properties calculated for specific subsets of materials in the database, including elastic²¹, thermoelectric²², piezoelectric²³, and dielectric²⁴ properties. It also includes a collection of apps such as a Pourbaix diagram calculator²⁵, and the underlying data are accessible via an API²⁶. Finally, the Open Quantum Materials Database (OQMD) contains calculations of a large number of hypothetical compounds based on structural prototypes^{27–29}, and provides tools for the construction of DFT ground state phase diagrams at ambient and high-pressure^{30–32}. The OQMD provides the entirety of the underlying database to download all at once, and a RESTful API for programmatic access³³.

We query all three databases for the calculated properties of materials whose crystal structures were sourced from the ICSD and aggregate them onto the Citrination platform³⁴ after converting records from all sources into a unified, consistent data format, the Physical Information File (PIF)³⁵. We then generate a set of comparable records for each pairwise combination of the databases—all calculations using the same initial crystal structure, by matching their ICSD Collection Codes (hereafter referred to as “ICSD ID”). In instances where more than one calculation within a single database was labeled with the same ICSD ID, we use the lowest energy calculation for all analysis. In addition, we discard records with obviously unphysical property values, and normalize properties to the same units, where required. We then perform statistical analysis on the final curated set of comparable records across the three databases. Definitions of the metrics used in our analysis are given in Appendix A, and details of the query and curation steps are provided in Section II of the Supplementary Information.

III. RESULTS

The aggregation and processing of the data from the three HT-DFT databases results in a set of $\sim 70,000$ total comparable DFT calculations. For each property of interest, i.e., formation energy per atom, volume per atom, band gap, total magnetization per formula unit (f.u.), the counts of records, and overlapping records for each pair of databases are shown in Table I. Approximately 15,000–25,000 comparisons can be made for each property and database pair, except for comparisons to formation energies from AFLOW, where only $\sim 2,200$ records are reported. As mentioned earlier, overlapping records across databases were determined by using exact ICSD ID matches for the reported calculations.

A. Overall pairwise comparison statistics

Table II shows some overall statistics for comparisons of all properties across comparable records in the three

	AFLOW	MP	OQMD	AFLOW-MP	AFLOW-OQMD	MP-OQMD
Formation Energy	2196	34907	22248	2070	1717	19082
Volume	21929	34907	22248	19258	15857	19082
Band Gap	21921	34907	22169	19253	15790	19007
Total Magnetization	21929	34907	22248	19258	15857	19082

TABLE I. The number of records after establishing ICSD ID equivalency for each property of interest in the AFLOW, Materials Project (MP), and OQMD HT-DFT databases, as well as for pairwise comparisons of the three databases.

databases: the median absolute difference (MAD), the interquartile range (IQR), the Pearson correlation coefficient (r), and Spearman’s rank correlation coefficient (ρ) (definitions of the metrics are in Appendix A). For band gap and total magnetization, the statistics were calculated only on subsets of overlapping records where both databases agreed that a material is non-metallic ($E_g > 0$) and is magnetic ($M > 0$), respectively.

Overall, we find that: (a) The MAD in formation energy across pairs of databases can be up to 0.105 eV/atom, comparable to the \sim 0.1 eV/atom difference between DFT and experimental formation energies¹². (b) The MAD in volume across pairs of databases can be up to $0.65 \text{ \AA}^3/\text{atom}$ (median absolute difference relative to mean (MRAD), of 3.8%), comparable to error between DFT and experiment³⁶. (c) The MAD in band gap across pairs of databases can be up to 0.21 eV, even when comparing only records where both databases agree that a material is not metallic. For around 5%–7% of overlapping records, databases disagree whether a material is metallic. (d) The comparison of total magnetization shows high variability across database pairs. While the dispersion of differences for the MP-OQMD comparison is very small (MAD of $0.01 \mu_B/\text{f.u.}$ and IQR of $0.05 \mu_B/\text{f.u.}$), the dispersion of differences in comparisons with AFLOW are rather large (up to MAD of $0.15 \mu_B/\text{f.u.}$ and IQR of up to $2.0 \mu_B/\text{f.u.}$). In all cases, the correlation between calculated values is lower than for the other three properties, with both Pearson and Spearman correlation coefficients ranging from 0.6–0.8. We further note that the latter poor correlation exists even after excluding overlapping records where the two databases disagree on whether the material is magnetic (10%–15% of the records).

B. Distribution of differences in calculated properties

We first analyze the raw differences in the calculated properties for records overlapping across pairs of databases. Figure 1 shows the distribution of the differences in calculated values for each of formation energy, volume, band gap, and total magnetization, for each pairwise combination of databases.

Formation energy: The distribution of differences in calculated formation energy across AFLOW-MP and

MP-OQMD is surprisingly bimodal, with peaks around 0 and ± 0.2 eV/atom. We find that the peak near 0.2 eV/atom in both pairwise comparisons corresponds mostly to oxides, and a difference in the reference chemical potential of oxygen used to calculate the formation energy. The chemical potential of oxygen in MP is \sim 0.4 eV/atom lower than that in AFLOW and OQMD. While the median difference ($\widetilde{\Delta x}$ in Figure 1) are reasonably small across all three pairwise comparisons (up to \sim 0.074 eV/atom), the difference distributions for AFLOW-MP and MP-OQMD are rather wide. The median absolute difference (MAD) and the interquartile range (IQR), both robust measures of the spread of a distribution, are up to \sim 0.105 eV/atom and \sim 0.173 eV/atom, respectively.

Volume: The distribution of differences in calculated volumes is skewed towards smaller volumes in the OQMD, but such a skew is absent in the AFLOW-MP comparison. Correspondingly, the median difference between AFLOW and MP volumes are \sim 0.01 $\text{Å}^3/\text{atom}$, whereas the median differences are \sim 0.62 $\text{Å}^3/\text{atom}$ and \sim 0.47 $\text{Å}^3/\text{atom}$ for AFLOW-OQMD and MP-OQMD, respectively. The consistently smaller volumes calculated in the OQMD can be understood to result from the choice of the plane wave energy cutoff used for DFT relaxation calculations. The OQMD chooses a plane wave cutoff that is lower than that used in AFLOW and MP (ENMAX in the POTCAR file, up to 400 eV in OQMD, as opposed to 520 eV in MP and up to 560 eV in AFLOW) for full cell relaxations. The lower plane wave cutoff results in Pulay stresses and generally smaller volumes than fully relaxed calculations. The MAD in volumes for comparisons, especially for OQMD with the other two databases, is up to \sim 0.65 $\text{Å}^3/\text{atom}$.

Band gap: The distribution of differences in the calculated band gaps is slightly skewed towards larger band gaps in the OQMD, but this skew is absent in the AFLOW-MP comparison. Correspondingly, the median difference in band gaps between AFLOW and MP is \sim 0.01 eV, and up to \sim 0.14 eV for comparisons with OQMD. The larger band gaps calculated in the OQMD can be partially understood to also result from the choice of lower plane wave energy cutoffs. Phenomenological theory suggests that a decrease in volume or interatomic distance results in a higher repulsive potential experienced by electrons, resulting in larger band gaps³⁷. This

	AFLW-MP				AFLW-OQMD				MP-OQMD			
	MAD	IQR	r	ρ	MAD	IQR	r	ρ	MAD	IQR	r	ρ
Formation Energy (eV/atom)	0.105	0.173	0.99	0.99	0.019	0.036	0.99	0.99	0.087	0.168	0.99	0.99
Volume ($\text{\AA}^3/\text{atom}$)	0.180	0.389	0.98	0.99	0.647	1.117	0.97	0.97	0.512	0.902	0.98	0.98
Band Gap (eV)*	0.078	0.203	0.94	0.92	0.209	0.364	0.92	0.91	0.178	0.277	0.93	0.92
Total Magnetization ($\mu_B/\text{f.u.}$)*	0.015	0.759	0.77	0.75	0.149	2.001	0.60	0.56	0.012	0.052	0.80	0.74

TABLE II. Overall statistics (median absolute difference (MAD), interquartile range (IQR), Pearson’s linear correlation coefficient (r), and Spearman’s rank correlation coefficient (ρ)) for the comparison of properties across HT-DFT databases. For each property, records overlapping across a pair of databases are compared (* for band gap and magnetization, only non-zero values are compared). Generally, lower MAD, lower IQR, higher r , and higher ρ values indicate better reproducibility of calculated properties.

increase in band gaps with compressive strains has been observed in experiment, e.g., for semiconductors³⁸. In addition, the spread in the differences in calculated band gaps is quite large: with an MAD of up to ~ 0.21 eV and an IQR of up to ~ 0.36 eV for comparisons with OQMD. The spread may be, in addition to the choice of energy cutoff as discussed above, due to the different ways in which the databases calculate the band gap. For example, OQMD calculates band gap from the electronic density of states (DOS), in contrast to AFLOW and MP which calculate it from band dispersions. The energy grid used for the calculation of DOS and/or k -point meshes used for band structure calculations can also have a notable effect on the precision and accuracy of the reported band gap.

Total magnetization: The median differences in AFLOW-MP and MP-OQMD are nearly zero, with reasonably small MAD values as well. However, the differences between the magnetization reported in AFLOW and the other two databases skew towards larger values in AFLOW, with long tails and correspondingly large dispersions. The difference between AFLOW and OQMD, in particular, shows an MAD of $\sim 0.15 \mu_B/\text{atom}$ and an IQR of $\sim 2.0 \mu_B/\text{atom}$. Further, as noted earlier, a significant fraction of 10–15% overlapping records across databases disagree on whether the material has non-zero total magnetization. This disagreement may in part be due to different pseudopotential choices for various elements (and correspondingly different number of valence electrons), and sampling of different magnetic configurations (e.g., ferrimagnetic and antiferromagnetic configurations are calculated in MP and AFLOW for a subset of compounds, in addition to the ferromagnetic state calculated in the OQMD).

C. Rank-order comparisons across properties

We next seek to make comparisons *across* properties. Instead of comparing the raw values of the properties directly, we compare overlapping records using the ordinal rank of the property in each database being compared (hereafter, referred to as “percentile rank”). Comparing

the percentile ranks of the properties has a few advantages: (a) It allows for a single consistent metric for comparison across all four properties regardless of the magnitude of the actual value and physical units. (b) It is not affected by many systematic differences, e.g., a constant shift of 0.1 eV in all calculated band gaps in one database. Such constant shifts in calculated properties do not affect the internal consistency of a HT-DFT database, and the percentile ranks which are similarly unaffected capture this property. (c) It is a robust, uniform, identifier of outliers in calculated properties.

Figure 2 consists of percentile rank scatterplots (closely related to the quantile-quantile or Q-Q plots) of each property of interest for each database pair. Note that for band gap (total magnetization), we only include overlapping records where the two databases being compared both report the material to be non-metallic (magnetic), to avoid having to rank near-zero or zero values against one another. A compact line along the diagonal corresponds to perfect correlation between the ranked properties, with more diffuse scattering indicating lower levels of correlation.

Formation energy: Of the four properties, formation energy shows the best correlation between each database pair, consistent with all r and ρ values close to 0.99 in Table II. Nonetheless, there is some off-diagonal scatter for the MP-OQMD comparison for larger (more positive) values of formation energy that is not found in the other database pairs. These calculations correspond to compounds with smaller (positive) formation energies, where the precision necessary to reliably rank the structure approaches the accuracy of the calculation.

Volume: The percentile rank comparison of volume shows higher off-diagonal scatter than that seen in comparisons of formation energy. There is a skew towards higher volumes in AFLOW and MP when compared to OQMD (scatter towards top-left of the diagonal in the AFLOW-OQMD and MP-OQMD comparisons), consistent with the discussion around plane wave energy cutoffs in the previous section.

Band gap: The percentile rank comparison of band

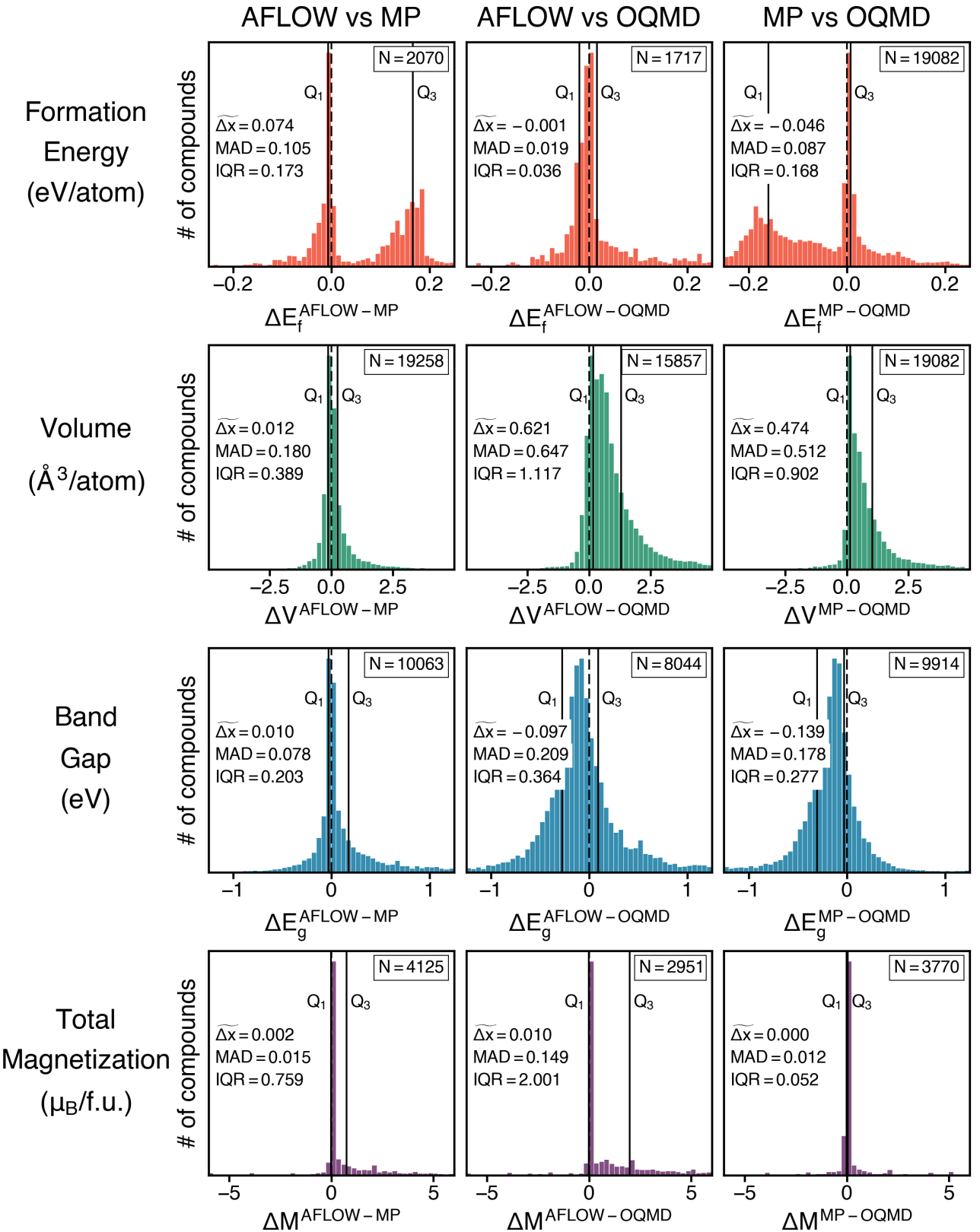


FIG. 1. Distribution of the differences in calculated properties across HT-DFT databases. Each panel corresponds to a property and pair of databases being compared. Solid vertical black lines correspond to the first (Q_1) and third (Q_3) quartiles of the distribution. The number of records overlapping across the two databases is shown in the top right corner of each panel; the median of distribution ($\tilde{\Delta}x$), the median absolute difference (MAD), and the interquartile range (IQR) are noted on the left.

gap shows even higher off-diagonal scatter than that observed in comparisons of both formation energy and volume. In particular, there is meaningful scatter *along the axes*, corresponding to cases where one database predicts the material to have a near-zero band gap whereas the other database predicts a (much larger) non-zero band gap.

Total magnetization: The percentile rank comparison of total magnetization per formula unit in all three pairwise comparisons shows a few distinct clusters along the diagonal, corresponding to nominally integer values of magnetic moment per formula unit. There is considerable off-diagonal “bowing” in the comparisons with AFLOW, consistent with the distribution of differences between AFLOW and the other two databases showing a skew towards larger magnetizations in AFLOW *and* long tails (lower panel in Figure 1). In addition, there is considerable off-diagonal scatter (horizontal and vertical bands in the magnetization panel of Figure 2) indicating significant disagreement between the values reported in the two databases.

Overall, a comparison of rank-ordered properties across two databases shows that formation energies and volumes are more easily reproduced than band gaps and total magnetizations, consistent with correlation coefficients decreasing from ~ 0.99 for formation energy to ~ 0.6 for total magnetization (Table II).

D. Reproducibility across materials classes

Intuitively, we expect the level of agreement among the databases to be a strong function of materials class. Therefore, we compare specific subsets of calculations based on various materials classes to elucidate potential causes of differences. The materials classes are defined based on chemical composition, the number of elemental components, the presence of magnetism, band gap, pseudopotential choices, and space group, as summarized in Table III. For classes defined by the output of a calculation (i.e., those based on magnetization and band gap), comparisons are only made if both databases agree that the property has a non-zero value.

Figure 3 contains the median absolute difference relative to the mean (MRAD) values for pairwise comparisons between databases, divided into materials classes as defined in Table III. Cells are colored based on the MRAD value listed. Empty cells correspond to trivial comparisons (e.g., values of band gap where both database agree the structure is metallic). We use MRAD as the metric here to reduce the effect of outliers (as compared to calculating means) as well as to enable comparisons across properties using the same metric. Overall, HT-DFT volumes show the best agreement (lowest MRAD values), from 1–4%. Band gaps show the worst overall agreement (highest MRAD values), 4–10%

across all pairwise comparisons. Formation energy comparisons with MP show MRAD values up to 6%, but the AFLOW-OQMD MRAD is only 1.3%. MRAD values for total magnetization vary highly from 0.5% for comparisons with MP to 7.6% for AFLOW-OQMD. In all cases, certain materials classes have distinctly higher or lower MRAD when compared to the MRAD averaged over all materials classes.

Formation Energy: In the comparisons with AFLOW, two materials classes, “Halides” and “Disagree on Metallic”, show the highest MRAD values of up to 14% and 40%, respectively. The high MRAD in halide formation energies can be understood to result from post hoc corrections to the elemental reference energies performed in MP and OQMD, but not in AFLOW, for the halide group of elements (see discussion in Section IVB). The high MRAD of the “Disagree on Metallic” class is likely an artifact of the small formation energies of the few records (~ 30 –50) in the comparison. As noted earlier, since AFLOW reports notably fewer formation energy values than the other databases, the comparisons are made with a much smaller set of records ($\sim 2,000$). Therefore, we ignore here some of the MRAD outliers in cases where the number of records being compared is very small (e.g., the material class “Magnetic” shows an MRAD of 13% between AFLOW and MP but there are only 5 records in the comparison). Further, the formation energies dataset has very few transition metal, rare-earth, and actinide element-containing compounds (Figures S2 and S6). New, different insights are likely to result from a larger dataset. In the MP-OQMD comparison, with a much larger comparable dataset ($\sim 19,000$), the “Nitride”, “Pnictide”, and “Chalcogenide” material classes show the highest MRAD values, 14%, 8%, and 11% respectively. This is partly due to differences in fitted elemental chemical potentials for pnictogen and chalcogen elements in MP and OQMD (Section IVB).

Volume: The best agreement is observed in the AFLOW-MP comparisons, with only the “Actinide” material class showing an MRAD greater than 2%. For comparisons with OQMD, the MRAD in volume is generally higher—due to the choice of lower plane wave energy cutoff used for cell relaxation, as discussed earlier (Section IIIB). The highest MRAD values in the comparisons with OQMD volumes are for the “Nitride” and “Halide” classes (~ 7 –9%). The default plane wave energy cutoffs in the VASP PAW potentials (ENMAX parameter) for N and F are among the highest (400 eV) of all elements. Thus, the lower energy cutoff used by OQMD for relaxation impacts the calculated volumes of nitrides and fluorides the most (Figures S7 and S11). Another material class, “Triclinic”, shows similarly high MRAD values of $\sim 8\%$ in comparisons with OQMD. Upon examination, we find that most triclinic materials in the comparisons are oxides, nitrides, and halides, and thus the high MRAD values are due to the chemical

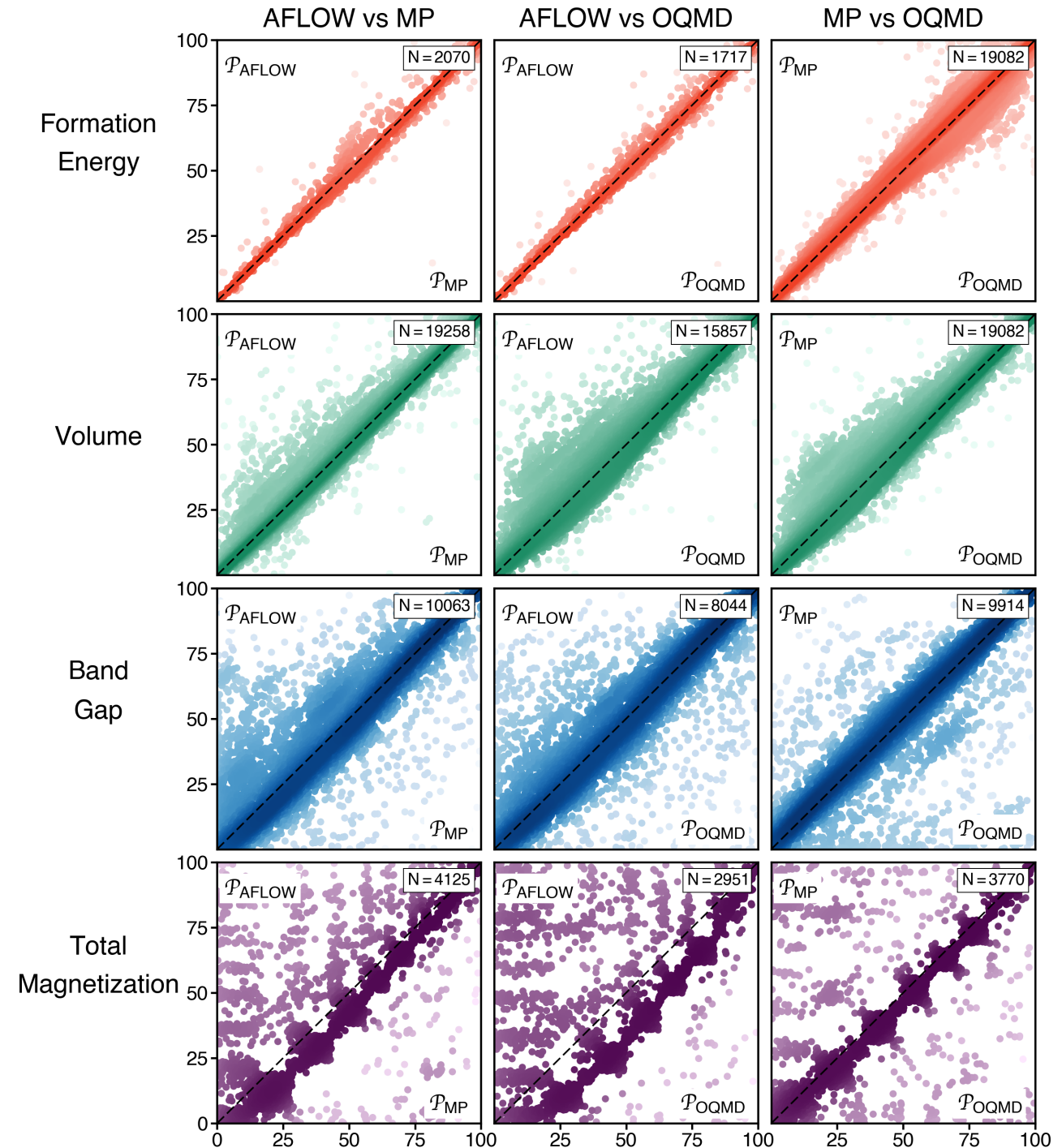


FIG. 2. Comparison of the calculated properties (formation energy, volume, band gap, and total magnetization) over records overlapping across pairwise combinations of HT-DFT databases plotted as a percentile rank. Overall, formation energies and volumes show better reproducibility than band gaps and magnetizations. The clusters seen in the magnetization comparisons correspond to nominally integer values of magnetic moments.

composition of these compounds rather than their crystal symmetry.

Band gap: While band gap comparisons show the highest MRAD values across properties, some materials

classes in particular show MRAD values much greater than $\sim 10\%$. Of these, in the “Intermetallic” and “Semiconductor” material classes, the MRAD values are expectedly high due to small average band gaps relative to which differences are reported, even though the

Class	Definition
Oxide	Contains O
Nitride	Contains N
Pnictide	Contains a group 15 element
Chalcogenide	Contains a group 16 element, except O
Halide	Contains a group 17 element
Alkali Metal	Contains a group 1 element, except H
Alkaline Earth Metal	Contains a group 2 element
Transition Metal	Contains a <i>d</i> -block element
Metalloid	Contains B, Si, Ge, As, Sb, or Te
Rare-Earth	Contains an element from the lanthanide series
Actinide	Contains an element from the actinide series
Metal-Nonmetal	Contains at least one metal element <i>and</i> at least one of C, N, O, F, P, S, Cl, Se, Br, I
Intermetallic	Contains only metallic elements
Magnetic	Both databases report a net magnetic moment $> 10^{-2} \mu_B/\text{f.u.}$
Non-magnetic	Both databases report no net magnetic moment $> 10^{-2} \mu_B/\text{f.u.}$
Disagree on Magnetic	The two databases disagree on whether a net magnetic moment $> 10^{-2} \mu_B/\text{f.u.}$ is present
Metallic	Both databases predict a band gap of $< 10^{-2} \text{ eV}$
Semiconductor	Both databases predict a band gap between 10^{-2} and 1.5 eV
Insulator	Both databases predict a band gap larger than 1.5 eV
Disagree on Metallic	The two databases disagree on whether a band gap $< 10^{-2} \text{ eV}$ is present
Pseudopotentials Agree	Both databases use the same set of pseudopotentials for all elements
Pseudopotentials Disagree	The databases use different pseudopotentials for at least one element
Elements	Contains only one element
Binaries	Contains two elements
Ternaries	Contains three elements
Quaternaries	Contains four elements
Triclinic	Space group 1–2
Monoclinic	Space group 3–15
Orthorhombic	Space group 16–74
Tetragonal	Space group 75–142
Trigonal	Space group 143–167
Hexagonal	Space group 168–194
Cubic	Space group 195–230

TABLE III. Definitions for the materials classes in used in this work.

absolute differences themselves are not conspicuously large (Figure S1). In other cases, the high MRAD values are a result of (a) different pseudopotential choices for elements (e.g., Cu/Cu_pv, Ce/Ce_3, Eu/Eu_2 choices in the “Disagree on Magnetic” class for the MP-OQMD comparison with an MRAD of $\sim 53\%$; see Figure S12), (b) using the GGA or GGA+*U* approach to calculate properties (e.g., for the “Actinide” material class with MRAD of up to 43% in comparisons with MP), or a combination of both factors (e.g., for the “Magnetic” material class with an MRAD of up to 27% in comparisons with AFLOW). Further discussions of these parameter choices are in Section IV.

Total magnetization: While MRAD values in the MP-OQMD comparison are generally small ($< 5\%$), some material classes show much higher MRAD values, especially in comparisons with AFLOW. As in the case of band gap values, we find these comparisons to be influenced by pseudopotential choice (of rare-earth elements in particular), GGA+*U*, or both (e.g., the “Metalloid” and “Rare-Earth” material classes in the

AFLOW-OQMD comparisons, “Intermetallic” and “Metallic” classes in the AFLOW-MP and AFLOW-OQMD comparisons). We note that some other material classes show high MRAD values, e.g., “Element”, “Binary”, “Ternary”, “Tetragonal”, “Hexagonal”, and “Cubic” (up to MRAD values up to $\sim 50\%$) due to, upon further examination, the parameter choices discussed above rather than due to number of components in the compound or crystal symmetry.

Finally, we investigated whether our results hold on a larger comparison set generated by linking very similar ICSD entries by using the crystal structure matching algorithm employed by the Materials Project (see Section II in the Supplementary Information). While some of the quantitative metrics we report varied by a few percent in the expanded comparison, the overall conclusions remain unchanged.

AFLOW vs MP				AFLOW vs OQMD				MP vs OQMD				
	ΔE_f	V	E_g	ΔE_f	V	E_g	M	ΔE_f	V	E_g	M	
All	5.8 (2070)	1.0 (19258)	3.8 (10063)	0.5 (4125)	1.3 (1717)	3.8 (15857)	8.9 (8044)	7.6 (2951)	6.3 (19082)	2.9 (19082)	8.0 (9914)	0.5 (3770)
Oxide	6.3 (989)	0.6 (6468)	3.3 (5289)	0.1 (1694)	1.0 (818)	5.8 (5269)	8.2 (4208)	0.1 (1159)	6.8 (6616)	5.7 (6616)	8.1 (5300)	0.0 (1601)
Nitride	0 (0)	1.2 (1639)	2.1 (1193)	0.3 (218)	0 (0)	9.3 (1257)	8.2 (936)	16.4 (149)	14.5 (1422)	6.9 (1422)	7.0 (1068)	0.6 (199)
Pnictide	6.4 (727)	0.9 (5470)	2.7 (3520)	0.3 (919)	2.3 (611)	4.5 (4330)	9.0 (2735)	2.5 (594)	8.2 (5210)	3.6 (5210)	8.1 (3385)	0.4 (805)
Chalcogenide	4.2 (412)	1.0 (3985)	4.8 (2982)	0.1 (714)	1.5 (340)	3.3 (3154)	8.6 (2328)	0.8 (470)	10.6 (3951)	2.3 (3951)	7.4 (2924)	0.2 (623)
Halide	14.1 (298)	1.0 (3850)	2.8 (3291)	0.0 (891)	10.7 (245)	8.7 (3107)	8.1 (2565)	0.1 (567)	7.8 (3700)	8.1 (3700)	6.7 (3029)	0.0 (726)
Alkali Metal	5.5 (695)	0.7 (4541)	2.9 (3605)	0.0 (897)	1.3 (599)	5.2 (3887)	9.4 (3019)	0.1 (618)	6.6 (4961)	5.0 (4961)	8.4 (3904)	0.0 (860)
Alkaline Earth Metal	4.8 (709)	0.5 (3448)	1.7 (2002)	0.1 (621)	0.8 (580)	3.1 (2929)	8.4 (1614)	0.3 (466)	5.7 (3398)	3.2 (3398)	8.1 (1960)	0.1 (575)
Transition Metal	4.9 (393)	1.1 (13028)	10.1 (5342)	0.8 (3595)	1.0 (313)	3.4 (10669)	10.8 (4176)	7.7 (2773)	5.7 (12500)	2.2 (12500)	8.4 (5025)	0.4 (3447)
Metalloid	5.7 (1063)	0.8 (6004)	2.0 (2965)	3.8 (979)	1.0 (856)	2.5 (4926)	8.6 (2330)	42.8 (637)	4.5 (5933)	1.6 (5933)	8.4 (2879)	1.8 (768)
Rare-Earth	3.0 (63)	1.1 (4630)	9.1 (1236)	3.9 (1229)	0.6 (48)	2.0 (3974)	9.9 (1038)	121.1 (651)	4.8 (5511)	1.3 (5511)	8.5 (1610)	12.0 (977)
Actinide	9.7 (4)	3.2 (670)	36.4 (222)	8.5 (300)	4.7 (4)	5.5 (569)	9.9 (167)	10.7 (272)	6.3 (758)	1.3 (758)	43.0 (233)	1.8 (438)
Metal-Nonmetal	5.8 (1246)	0.8 (12270)	4.5 (6717)	0.1 (3053)	1.2 (1035)	4.9 (10020)	8.9 (7004)	0.1 (2129)	7.4 (12374)	4.4 (12374)	7.9 (8690)	0.1 (2829)
Intermetallic	4.7 (182)	1.4 (3056)	20.4 (50)	41.2 (528)	2.7 (157)	1.6 (2882)	36.3 (35)	81.1 (404)	3.4 (2910)	1.2 (2910)	42.7 (54)	12.4 (446)
Magnetic	5.5 (12)	1.4 (4125)	27.4 (1580)	0.5 (4125)	13.0 (5)	5.6 (2951)	24.4 (1013)	7.6 (2951)	6.4 (3770)	3.4 (3770)	13.5 (1330)	0.5 (3770)
Non-Magnetic	5.8 (1991)	0.8 (13119)	2.3 (8106)	0 (0)	1.3 (1680)	3.2 (10520)	7.9 (6522)	0 (0)	6.2 (12922)	2.8 (12922)	7.3 (8146)	0 (0)
Disagree On Magnetic	5.1 (67)	1.3 (2014)	17.0 (377)	0 (0)	1.8 (32)	2.8 (2886)	18.9 (509)	0 (0)	6.7 (2390)	2.6 (2390)	53.1 (438)	0 (0)
Metallic	2.4 (498)	1.3 (7951)	0 (0)	32.0 (1888)	1.6 (436)	1.7 (6765)	0 (0)	67.3 (1508)	3.7 (8092)	1.0 (8092)	0 (0)	5.1 (2066)
Semiconductor	4.6 (472)	0.7 (2456)	11.9 (2456)	0.1 (394)	2.6 (328)	2.3 (1743)	17.9 (1743)	0.1 (231)	7.7 (2400)	2.3 (2400)	16.5 (2400)	0.0 (445)
Insulator	6.0 (1032)	0.7 (6785)	1.8 (6785)	0.0 (751)	1.0 (855)	6.4 (5577)	6.9 (5577)	0.0 (500)	7.1 (6791)	6.2 (6791)	6.4 (6791)	0.0 (656)
Disagree On Metallic	15.8 (47)	1.5 (1239)	0 (0)	0.3 (656)	39.2 (32)	5.9 (981)	0 (0)	0.4 (419)	7.1 (1001)	3.9 (1001)	0 (0)	0.1 (361)
Pseudopotentials Agree	5.7 (1547)	0.9 (11410)	3.3 (6621)	0.2 (2571)	1.5 (1139)	4.4 (5635)	7.3 (3793)	2.4 (453)	6.6 (10616)	3.3 (10616)	7.5 (6604)	1.6 (980)
Pseudopotentials Disagree	5.8 (523)	1.1 (7848)	4.9 (3442)	4.3 (1554)	1.0 (578)	3.5 (10222)	10.6 (4251)	9.1 (2498)	5.9 (8466)	2.5 (8466)	9.2 (3310)	0.3 (2790)
Element	8.1 (91)	1.5 (159)	2.4 (45)	12.4 (8)	5.3 (76)	2.1 (149)	7.9 (33)	27.6 (5)	9.9 (152)	2.3 (152)	6.4 (42)	4.5 (6)
Binary	5.8 (648)	1.4 (3532)	3.0 (975)	17.7 (492)	1.8 (542)	2.6 (2698)	8.6 (790)	46.5 (377)	6.9 (2934)	1.7 (2934)	7.2 (877)	5.1 (438)
Ternary	5.5 (1003)	1.0 (10319)	4.0 (4526)	4.3 (2229)	1.3 (841)	2.9 (8706)	8.5 (3720)	25.4 (1665)	5.5 (10423)	1.8 (10423)	8.2 (4443)	1.3 (2025)
Quaternary	5.8 (308)	0.7 (4270)	3.9 (3530)	0.1 (1130)	0.6 (250)	5.4 (3438)	8.3 (2786)	0.1 (725)	6.7 (4497)	4.9 (4497)	8.0 (3630)	0.1 (1022)
Triclinic	6.0 (104)	0.9 (1003)	3.9 (902)	0.1 (216)	1.2 (89)	8.6 (805)	7.6 (714)	0.1 (132)	8.3 (1052)	7.5 (1052)	7.4 (930)	0.0 (207)
Monoclinic	6.0 (446)	0.9 (3691)	3.8 (2991)	0.1 (764)	1.7 (373)	6.1 (2991)	8.5 (2340)	0.1 (491)	7.5 (4052)	5.3 (4052)	7.6 (3178)	0.0 (738)
Orthorhombic	5.8 (507)	0.9 (4550)	3.7 (2552)	0.3 (746)	1.3 (405)	3.2 (3625)	8.8 (1953)	2.2 (522)	5.7 (4634)	2.5 (4634)	8.0 (2509)	0.4 (724)
Tetragonal	5.8 (246)	1.0 (2797)	5.0 (1042)	5.9 (641)	1.2 (202)	3.0 (2369)	10.0 (861)	38.2 (496)	5.1 (2762)	1.9 (2762)	8.8 (960)	2.4 (572)
Trigonal	5.4 (241)	0.9 (1746)	3.5 (1144)	0.1 (389)	0.9 (199)	3.9 (1404)	9.7 (896)	0.1 (285)	6.8 (1507)	3.5 (1507)	8.0 (947)	0.1 (326)
Hexagonal	4.7 (196)	1.0 (2108)	3.3 (545)	11.3 (427)	0.8 (158)	1.9 (1626)	8.8 (438)	49.8 (231)	4.2 (1798)	1.2 (1798)	9.0 (440)	3.3 (339)
Cubic	5.7 (295)	1.1 (2988)	2.9 (752)	20.7 (795)	1.5 (217)	2.6 (2203)	10.6 (527)	38.6 (541)	5.4 (2343)	1.4 (2343)	9.2 (600)	2.8 (557)

FIG. 3. Median percent absolute differences between properties (formation energy, volume, band gap, total magnetization) calculated in the three databases (AFLOW, MP, OQMD), compared two at a time, across various classes of materials as defined in Table III. The numbers in parentheses indicate the number of overlapping records belonging to the respective material class for a given pair of databases. Trivial comparisons are left blank (e.g., the difference in total magnetization for non-magnetic compounds).

IV. DISCUSSION

We discuss some of the most important factors affecting the differences across HT-DFT calculations of properties below. Some of the other factors that either have a minor effect (e.g., *post hoc* calculation of band gap from band dispersions or density of states) or are specific to a database/property (e.g., plane wave cutoff energy for full cell relaxations in OQMD) have been discussed in the earlier sections.

A. Effects of pseudopotential choice

For nearly all elements, VASP provides multiple PAW potentials to choose from, with different numbers of electrons in the valence. The choice of pseudopotential varies across the HT-DFT databases due to factors such as changes in VASP recommendations and issues of calculation convergence or reproduction of experimental thermochemical data^{39,40}. Interestingly, the choice of pseudopotential has minimal effect on the calculated formation energies and volumes (up to a difference of 1% in cases where pseudopotentials do or do not match; see rows “Pseudopotentials Agree” and “Pseudopotentials Disagree” in Figure 3). On the other hand, the number of valence electrons and consequently the choice of pseudopotential affects the calculated band gaps and magnetization values severely. Especially egregious differences across those properties in material classes such as “Rare-Earth” and “Magnetic” (Figure 3) can be directly traced to different pseudopotential choices. For rare-earth and actinide elements in particular, with *f*-electrons that are poorly described by DFT⁴¹, using pseudopotentials that treat *f*-electrons in core or valence can have a significant impact on the calculated band gap (e.g., “Intermetallic” and “Magnetic” classes in Figure 3) and magnetization (e.g., “Rare-Earth” and “Intermetallic” classes in Figure 3) values.

B. Elemental reference states

The largest disagreements in HT-DFT formation energies can be understood to result from different elemental reference states used across databases. To our knowledge, the formation energies reported in AFLOW use DFT total energies of the bulk elements as the reference states, whereas both MP and OQMD use reference energies that are fitted to experimental formation energies^{12,39}. Further, the latter case involves some more choices regarding how the fitted elemental references states are determined. (a) Should all elemental reference energies be fit to experimental data or only a subset? The OQMD fits only elements whose DFT ground states are poor representation of the experimental reference states (i.e., elements that are gases or that have a solid-solid phase transition below room temperature)¹², whereas MP fits all elemental

reference energies. (b) What experimental thermochemical data should be used for fitting, given a lack of a single, widely-accepted set of standard experimental dataset for solids? MP and OQMD use experimental formation energies from different sources to fit elemental reference energies^{12,40}, and this affects calculated formation energies even in cases where the same pseudopotential is used for the element in both databases (e.g., a reference energy of around -4.9 eV and -4.5 eV for O in MP and OQMD respectively). This effect of fitted elemental reference states is shown in the calculated formation energies averaged over compounds containing each element in Figures S2, S6, and S10.

C. GGA vs. GGA+U approach

One of the ways to treat the issue of over-delocalization in DFT is to use the DFT+*U* approach^{42,43} (or “GGA+*U*” when used with GGA). Similar to the case of fitting elemental references, using the GGA+*U* approach requires additional HT-DFT choices. (a) Whether or not to use GGA+*U* for calculating properties of a given material. All three HT-DFT databases have slightly different sets of compounds for which the GGA+*U* approach is applied. The OQMD uses GGA+*U* only for oxides of certain 3d transition metals (the V–Cu series) and actinide metals¹². MP uses GGA+*U* for oxides, fluorides, and sulfides of a larger set of transition metals, but not actinides⁴⁰. AFLOW applies it to an even larger set of compounds, nearly all those containing *d*- or *f*-block elements⁴⁴. (b) What effective *U* value should be used for each element? The three HT-DFT databases all use different effective *U* values for each element, obtained either from previous work (OQMD) or in-house parameterization by fitting to experimental data (AFLOW and MP)^{17,45}. Further, *post hoc* corrections are required to maintain consistency between formation energies calculated using the GGA and GGA+*U* approaches, especially in constructing phase diagrams involving compounds calculated using the two different approaches. Such corrections are obtained by fitting to experimental reaction energies, and can be different between HT-DFT databases based on the source of such reaction energies.

V. CONCLUSION

Recent years have seen a dramatic increase in the application of informatics methods for materials development, using high-throughput DFT data. Several prominent HT-DFT databases exist and each uses different input parameters and post-processing techniques to calculate materials properties. Quantifying the uncertainty in calculated properties due to such parameter choices is therefore crucial to understanding the reproducibility and interoperability of such data. In this work, we centralize data from three of the largest HT-DFT databases,

AFLW, Materials Project, and OQMD, into a common data platform, allowing records to be accurately compared. We then compare four properties—formation energy, volume, band gap, and total magnetization—of materials calculated in each of the HT-DFT databases using the same initial crystal structure.

Our comparisons show that formation energy and volume are more easily reproduced than band gap and total magnetization. Interestingly, we find that the average difference in calculated properties across two HT-DFT databases is comparable to that between DFT and experiment: up to 0.105 eV/atom for formation energy, 4% for volume, 0.21 eV for band gap, and 0.15 μ_B /formula unit for total magnetization. Further, certain input parameter choices disproportionately affect HT-DFT properties of particular classes of materials, e.g. choice of planewave cutoff on formation energies and volumes of oxides and halides, and the choice of pseudopotential on the band gaps and magnetization of rare-earth compounds.

As HT-DFT databases continue to mature, systematic comparisons and standardization of calculations are essential. In particular, we recommend efforts to standardize choices surrounding pseudopotentials, plane wave energy cutoffs, fitting elemental reference energies, using the GGA+ U approach, the effective U values used, and post-processing steps to obtain properties such as band gap from the electronic structure.

ACKNOWLEDGEMENTS

This material is based upon work supported by the U.S. Department of Energy, Office of Science, Office of Basic Energy Sciences, Small Business Technology Transfer Program under Award Number DE-SC0015106.

DATA AVAILABILITY

All data required to perform the analysis presented in this work are made available via the open Citrination platform (<https://citrination.com>). The individual datasets can be accessed at <https://citrination.com/datasets/187629> (AFLW), <https://citrination.com/datasets/188648> (Materials Project), and <https://citrination.com/datasets/187988> (OQMD).

Appendix A: Definitions of statistical quantities

The definitions of statistical quantities and their symbols used in this work throughout are as follows (x_i and y_i refer to the two sets of data being compared, e.g. from two different databases):

1. Median difference ($\widetilde{\Delta x}$):

$$\widetilde{\Delta x} = \text{median}(x_i - y_i) \quad (\text{A1})$$

2. Median absolute difference (MAD):

$$\text{MAD} = \text{median}(|x_i - y_i|) \quad (\text{A2})$$

3. Interquartile range (IQR):

$$\text{IQR} = Q_3 - Q_1 \quad (\text{A3})$$

where Q_1 and Q_3 are the first and third quartiles (25th and 75th percentiles), respectively.

4. Median relative absolute difference (MRAD):

$$\text{MRAD} = \text{median}\left(\frac{|x_i - y_i|}{|x_i + y_i|/2} \times 100\right) \quad (\text{A4})$$

5. Pearson correlation coefficient (r):

$$r(x, y) = \frac{\sum_i^n (x_i - \bar{x})(y_i - \bar{y})}{\sqrt{\sum_i^n (x_i - \bar{x})^2} \sqrt{\sum_i^n (y_i - \bar{y})^2}} \quad (\text{A5})$$

where $\bar{x} = \frac{1}{n} \sum_i^n x_i$ is the sample mean, and n is the sample size.

6. Spearman's rank correlation coefficient (ρ) is defined as the Pearson correlation coefficient between rank variables x_i^R and y_i^R corresponding to raw data values x_i and y_i , respectively:

$$\rho(x, y) = r(x^R, y^R) \quad (\text{A6})$$

* These authors contributed equally to this work

† bryce@citrine.io

- ¹ S. Curtarolo, G. L. Hart, M. B. Nardelli, N. Mingo, S. Sanvito, and O. Levy, *Nat. Mater.* **12**, 191 (2013).
- ² A. Jain, Y. Shin, and K. A. Persson, *Nat. Rev. Mater.* **1**, 15004 (2016).
- ³ J. E. Saal, S. Kirklin, M. Aykol, B. Meredig, and C. Wolverton, *JOM* **65**, 1501 (2013).
- ⁴ G. Kresse and J. Furthmüller, *Comput. Mater. Sci.* **6**, 15 (1996).
- ⁵ G. Kresse and J. Furthmüller, *Phys. Rev. B* **54**, 11169 (1996).
- ⁶ A. E. Mattsson, P. A. Schultz, M. P. Desjarlais, T. R. Mattsson, and K. Leung, *Modell. Simul. Mater. Sci. Eng.* **13**, R1 (2004).
- ⁷ Y. Zhuo, A. M. Tehrani, A. O. Oliynyk, A. C. Duke, and J. Brigo, *Nat. Commun.* **9**, 1 (2018).
- ⁸ B. Meredig, A. Agrawal, S. Kirklin, J. E. Saal, J. Doak, A. Thompson, K. Zhang, A. Choudhary, and C. Wolverton, *Phys. Rev. B* **89**, 094104 (2014).
- ⁹ K. Lejaeghere, G. Bihlmayer, T. Björkman, P. Blaha, S. Blügel, V. Blum, D. Caliste, I. E. Castelli, S. J. Clark, A. Dal Corso, *et al.*, *Science* **351**, aad3000 (2016).
- ¹⁰ S. Curtarolo, W. Setyawan, S. Wang, J. Xue, K. Yang, R. H. Taylor, L. J. Nelson, G. L. Hart, S. Sanvito, M. Buongiorno-Nardelli, *et al.*, *Comput. Mater. Sci.* **58**, 227 (2012).
- ¹¹ A. Jain, S. P. Ong, G. Hautier, W. Chen, W. D. Richards, S. Dacek, S. Cholia, D. Gunter, D. Skinner, G. Ceder, *et al.*, *APL Mater.* **1**, 011002 (2013).
- ¹² S. Kirklin, J. E. Saal, B. Meredig, A. Thompson, J. W. Doak, M. Aykol, S. Rühl, and C. Wolverton, *npj Comput. Mater.* **1**, 15010 (2015).
- ¹³ A. Belsky, M. Hellenbrandt, V. L. Karen, and P. Luksch, *Acta Crystall. B* **58**, 364 (2002).
- ¹⁴ P. E. Blöchl, *Phys. Rev. B* **50**, 17953 (1996).
- ¹⁵ G. Kresse and D. Joubert, *Phys. Rev. B* **59**, 1758 (1999).
- ¹⁶ J. P. Perdew, K. Burke, and M. Ernzerhof, *Phys. Rev. Lett.* **77**, 3865 (1996).
- ¹⁷ W. Setyawan and S. Curtarolo, *Comput. Mater. Sci.* **49**, 299 (2010).
- ¹⁸ O. Levy, G. L. Hart, and S. Curtarolo, *J. Am. Chem. Soc.* **132**, 4830 (2010).
- ¹⁹ C. Toher, J. J. Plata, O. Levy, M. de Jong, M. Asta, M. B. Nardelli, and S. Curtarolo, *Phys. Rev. B* **90**, 174107 (2014).
- ²⁰ R. H. Taylor, F. Rose, C. Toher, O. Levy, K. Yang, M. B. Nardelli, and S. Curtarolo, *Comput. Mater. Sci.* **93**, 178 (2014).
- ²¹ M. De Jong, W. Chen, T. Angsten, A. Jain, R. Notestine, A. Gamst, M. Sluiter, C. K. Ande, S. Van Der Zwaag, J. J. Plata, *et al.*, *Sci. Data* **2**, 150009 (2015).
- ²² W. Chen, J.-H. Pöhls, G. Hautier, D. Broberg, S. Bajaj, U. Aydemir, Z. M. Gibbs, H. Zhu, M. Asta, G. J. Snyder, *et al.*, *J. Mater. Chem. C* **4**, 4414 (2016).
- ²³ M. De Jong, W. Chen, H. Geerlings, M. Asta, and K. A. Persson, *Sci. Data* **2** (2015).
- ²⁴ I. Petousis, D. Mrdjenovich, E. Ballouz, M. Liu, D. Winston, W. Chen, T. Graf, T. D. Schladt, K. A. Persson, and F. B. Prinz, *Sci. Data* **4**, 160134 (2017).
- ²⁵ K. A. Persson, B. Waldwick, P. Lazic, and G. Ceder, *Phys. Rev. B* **85**, 235438 (2012).
- ²⁶ S. P. Ong, S. Cholia, A. Jain, M. Brafman, D. Gunter, G. Ceder, and K. A. Persson, *Comput. Mater. Sci.* **97**, 209 (2015).
- ²⁷ S. Kirklin, J. E. Saal, V. I. Hegde, and C. Wolverton, *Acta Mater.* **102**, 125 (2016).
- ²⁸ A. A. Emery, J. E. Saal, S. Kirklin, V. I. Hegde, and

- C. Wolverton, Chem. Mater. **28**, 5621 (2016).
- ²⁹ D. Wang, M. Amsler, V. I. Hegde, J. E. Saal, A. Issa, B.-C. Zhou, X. Zeng, and C. Wolverton, Acta Mater. **158**, 65 (2018).
- ³⁰ A. R Akbarzadeh, V. Ozoliņš, and C. Wolverton, Adv. Mater. **19**, 3233 (2007).
- ³¹ V. I. Hegde, M. Aykol, S. Kirklin, and C. Wolverton, Sci. Adv. **6**, eaay5606 (2020).
- ³² M. Amsler, V. I. Hegde, S. D. Jacobsen, and C. Wolverton, Phys. Rev. X **8**, 041021 (2018).
- ³³ “OQMD RESTful API,” <http://oqmd.org/static/docs/restful.html> (2019), accessed: May 2020.
- ³⁴ J. O’Mara, B. Meredig, and K. Michel, JOM **68**, 2031 (2016).
- ³⁵ K. Michel and B. Meredig, MRS Bull. **41**, 617 (2016).
- ³⁶ P. Haas, F. Tran, and P. Blaha, Phys. Rev. B **79**, 085104 (2009).
- ³⁷ G. Olsen, C. Nuese, and R. Smith, J. Appl. Phys. **49**, 5523 (1978).
- ³⁸ C. Kuo, S. Vong, R. Cohen, and G. Stringfellow, J. Appl. Phys. **57**, 5428 (1985).
- ³⁹ “Materials Project: Calculations Guide,” <https://materialsproject.org/docs/calculations>, accessed: December 2019.
- ⁴⁰ A. Jain, G. Hautier, C. J. Moore, S. P. Ong, C. C. Fischer, T. Mueller, K. A. Persson, and G. Ceder, Comput. Mater. Sci. **50**, 2295 (2011).
- ⁴¹ L. Eyring, K. A. Gschneidner, and G. H. Lander, *Handbook on the physics and chemistry of rare earths*, Vol. 32 (Elsevier, 2002).
- ⁴² V. I. Anisimov, J. Zaanen, and O. K. Andersen, Phys. Rev. B **44**, 943 (1991).
- ⁴³ H. J. Kulik, J. Chem. Phys. **142**, 240901 (2015).
- ⁴⁴ C. E. Calderon, J. J. Plata, C. Toher, C. Osés, O. Levy, M. Fornari, A. Natan, M. J. Mehl, G. Hart, M. B. Nardelli, and S. Curtarolo, Comput. Mater. Sci. **108**, 233 (2015).
- ⁴⁵ A. Jain, G. Hautier, S. P. Ong, C. J. Moore, C. C. Fischer, K. A. Persson, and G. Ceder, Phys. Rev. B **84**, 045115 (2011).

Supplementary Information for “Reproducibility in high-throughput density functional theory: a comparison of AFLOW, Materials Project, and OQMD”

Vinay I. Hegde,^{1,*} Christopher K. H. Borg,^{1,*} Zachary del Rosario,^{1,2} Yoolhee Kim,¹ Maxwell Hutchinson,¹ Erin Antono,¹ Julia Ling,¹ Paul Saxe,³ James E. Saal,¹ and Bryce Meredig^{1,†}

¹Citrine Informatics, 2629 Broadway, Redwood City, CA 94063

²Olin College of Engineering, 1000 Olin Way, Needham, MA 02492

³Molecular Sciences Software Institute, Virginia Tech, Blacksburg, VA 24061

(Dated: July 7, 2020)

I. HT-DFT DATABASES AND MANAGEMENT CODES

Given the popularity of DFT as a method generating materials data, a number of HT-DFT databases with various focus areas have emerged; a list of exemplars is given in Table I. Similarly, codes for the management of these databases, including the workflows to generate the data, have been developed by several groups around the world, such as the packages listed in Table II.

Database	Link	Materials	Properties	Reference
Aflowlib	materials.duke.edu/aflow.html	inorganic solids	electronic structure, thermodynamics	[1]
Alloy database	alloy.phys.cmu.edu	intermetallics	structure, cohesive energies	[2]
CatApp	slac.stanford.edu/~strabo/catapp	molecules on surfaces	reaction/activation energies	[3]
CCCBDB	cccbdb.nist.gov	atoms, molecules	thermochemical properties	[4]
CMR	cmr.fysik.dtu.dk	perovskites, 2D materials	energetics, electronic structure	[5]
CompES-X	compes-x.nims.go.jp	inorganic solids	electronic structure	
Crystallium	crystallium.materialsvirtuallab.org	elemental solids	surface, grain boundary energetics	[6]
CEP		organic photovoltaics	HOMO-LUMO energies	[7]
JARVIS-DFT	ctcms.nist.gov/~knc6/JVASP.html	2D/solid inorganics	elastic, thermoelectric properties	[8]
NRELMatDB	materials.nrel.gov	inorganic solids	quasiparticle energies	[9]
Materials Project	materialsproject.org	inorganic solids	mechanical, dielectric, piezoelectric	[10]
NoMaD	nomad-coe.eu	inorganic solids	raw DFT calculation files	
OQMD	oqmd.org	inorganic solids	energetics, electronic structure	[11]
phonondb	phonondb.mtl.kyoto-u.ac.jp	inorganic solids	phonons, thermal properties	
TE Design Lab		semiconductors	electronic, thermoelectric properties	[12]

TABLE I. A selection of publicly-available HT-DFT databases.

II. DATA MANAGEMENT

The primary challenge in comparing calculations from different HT-DFT databases is to collect the relevant database entries and determine equivalency between unique calculations of the same structure. This section outlines the workflow of ingesting data from AFLOW, Materials Project, and OQMD into a central repository (the Citrination platform²⁹), all post-extraction processing of the data, the method for querying the post-processed data from Citrination, and the method of determining whether two records were comparable.

A. Importing Data into Citrination

To create a complete and searchable system of records, entries from each HT-DFT database were imported into the Citrination platform²⁹, after standardization into the Physical Information File (PIF) format³⁰ using the `pypif`³¹ package. The data in this work represents the data found on the public-facing HT-DFT databases, aggregated in December 2019.

Each HT-DFT database was queried independently using their respective APIs:

Code	Functionality	Link	Reference
AFLOW	calculation setup, submission	High-throughput workflows materials.duke.edu/aflow.html	[13]
AiiDA	calculation setup, submission, storage	aiida.net	[14]
ASE	calculation setup, submission, analysis	wiki.fysik.dtu.dk/ase	[15]
MPInterfaces	surface calculation setup, analysis	github.com/henniggroup/MPInterfaces	[16]
pymatgen	calculation setup, analysis	pymatgen.org	[17]
qmpy	calculation setup, management, analysis	pypi.org/project/qmpy	[18]
Calculation of properties/model building			
Amp	atomistic potentials	amp.readthedocs.io	[19]
ATAT	cluster expansions	brown.edu/Departments/Engineering/Labs/avdw/atat	[20]
atomate	electronic structure, dielectric tensors	atomate.org	[21]
CALYPSO	crystal structure prediction	www.calypso.cn	[22]
MAST	defects, diffusion	pythonhosted.org/MAST	[23]
Mint	crystal structure utilities	github.com/materials/mint	
phonopy	phonons, high-temperature properties	atztogo.github.io/phonopy	[24]
SeeK-path	high-symmetry paths in Brillouin zone	materialscloud.org/work/tools/seekpath	[25]
SLUSCHI	melting temperatures	blogs.brown.edu/qhong/?page_id=102	[26]
USPEX	crystal structure prediction	uspex-team.org/en/uspex/overview	[27]
Xtalopt	crystal structure prediction	xtalopt.github.io	[28]

TABLE II. A selection of software tools for automating HT-DFT workflows and property calculations.

1. AFLOW: The query was performed using the AFLUX API¹, retrieving all records in the `icsd` catalog. The query resulted in 60,324 records, which were uploaded onto Citrination as PIF objects (<https://citrination.com/datasets/187629>).
2. Materials Project: The query was performed using the MPRester API³², retrieving all records with non-empty `icsd_ids` field. The query resulted in 48,833 records, which were uploaded onto Citrination as PIF objects (<https://citrination.com/datasets/188648>). In addition, some normalized properties such as per-atom volume and per-formula-unit magnetization that were not queried directly but calculated from queried data were added to the PIF objects prior to upload.
3. OQMD: The query was performed using qmpy and a version 1.2 of the underlying database, filtering on `FormationEnergy` objects associated with converged "static" `Calculation` objects and `Entry` objects with "icsd" in the "path" field. The query resulted in 37,989 records, which were uploaded onto Citrination as PIF objects (<https://citrination.com/datasets/187988>). In addition, some properties that were not directly queried but retrieved as metadata, such as labels of PAW potentials and crystal system, were added to the PIF objects prior to upload.

B. Querying Data from Citrination

The HT-DFT database-specific tags for each of the queried properties are given in Table III. The datasets uploaded onto the Citrination platform can all be queried using a common query language. The common query language enables properties from all three databases to be extracted using the same search key irrespective of the ingested field names. For instance, the number of atoms in the unit cell is extracted as `number_of_atoms` for all three databases despite varying labels (e.g., `nsites`, `natoms`, `calculation__output__natoms`) across databases.

C. Structure Equivalency

In order to perform a fair comparison between two HT-DFT databases, it is essential to generate a set of equivalent records for each pair of databases considered. We use the ICSD Collection Code(s) (hereafter, “ICSD ID(s)”) in the metadata of each entry to generate a set of comparable records.

Property	AFLOW	Materials Project	OQMD
Record ID	auid	material_id	entry_id
Record URL	aurl	-	-
Composition	compound	unit_cell_formula	composition__formula
Number of atoms	natoms	nsites	output__natoms
Total energy (/unit cell)	energy_cell	final_energy	calculation__energy
Total energy (/atom)	energy_atom	final_energy_per_atom	calculation__energy_pa
Formation energy	enthalpy_formation_atom	formation_energy_per_atom	formation__delta_e
Convex hull distance	-	e_above_hull	formation__stability
Volume (/unit cell)	volume_cell	volume	output__volume
Volume (/atom)	volume_atom	-	output__volume_pa
Magnetization (/unit cell)	spin_cell	total_magnetization	-
Magnetization (/atom)	spin_atom	-	calculation__magmom_pa
Band gap	Egap	band_gap	calculation__band_gap
Space group ITC #	spacegroup_relax	spacegroup	spacegroup__number
Crystal system	lattice_system_relax	crystal_system	-
Pseudopotentials	species_pp	pseudo_potential	calculation__settings

TABLE III. HT-DFT database-specific tags for properties compared in this work. In cases where they were not directly queried, normalized values such as per-atom values for “volume” and per-formula unit values for “total magnetization” were calculated from the non-normalized queried data.

1. Exact ICSD ID Matching

The main text contains analysis only for records with the exact same ICSD ID across the two databases being compared at a time, ensuring that the crystal structure of the materials being compared are the same.

2. Aliasing for Multiple ICSD IDs Per Record

Since the former process of exact ICSD ID matching results in a smaller set of records (less than 50%) when compared to the total ICSD entries in each database, we investigated if our results hold on a larger comparison set generated by linking similar ICSD entries. For the process of linking similar ICSD entries, we use the structure comparison and matching algorithm implemented within the Materials Project. The process involves the following two steps:

STEP 1. Annotation of extracted data with “ICSD UID”

1. *Generation of a set of ICSD UIDs from Materials Project:* An ICSD UID is defined as a set of ICSD Collection Codes (ICSD IDs) belonging to the same material. Materials Project already groups ICSD IDs per material, but imperfectly. For example, there are three different records for AgO in Materials Project that share the ICSD ID 60625 (https://citrination.com/datasets/187464/show_search?searchMatchOption=fuzzyMatch&systemIdValue=605625). This task in the curation pipeline thus aggregates the ICSD IDs from all three such records to generate a super “ICSD UID”. For instance, GaN (mp-830) was associated with 10 ICSD IDs, and the corresponding ICSD UID is the set of all 10 ICSD IDs: “187047–190412–67781–156260–41546–157511–248504–191770–185155–290614”.
2. *Annotation of extracted records with an ICSD UID:* First, every record retrieved from Materials Project is matched to an ICSD UID from the set above, depending on the ICSD IDs in the record (the set of ICSD IDs in the record will be a subset of exactly one ICSD UID). Second, it is attempted to match every record retrieved from AFLOW and OQMD to ICSD UID. If no match is found, the ICSD ID in such a record constitutes a new ICSD UID.

The resulting extracted properties dictionary has the following format:

```
{
  AFLOW: [
    {
      db_id: 1,
```

```

    prop_name_1: prop_val_1,
    prop_name_2: prop_val_2,
    icsd_uid: icsd_id_1-icsd_id_6-icsd_id_7,
    ...
},
{
    db_id: 2,
    icsd_uid: icsd_id_2-icsd_id_3,
    ...
},
{
    db_id: 3,
    icsd_uid: icsd_id_1-icsd_id_6-icsd_id_7,
    ...
},
...
...
],
MP: [
    ...
    ...
],
...
}

```

STEP 2. Reverse-mapping properties to ICSD UIDs

This step involves “inverting” the dictionary of extracted properties above such that the ICSD UIDs are the keys and a list of data records corresponding to each UID is the value. The inverted dictionary at this step has the following format:

```

{
    AFLOW: {
        icsd_id_1-icsd_id_6-icsd_id_7: [
            {
                db_id: 1,
                prop_name_1: prop_val_1,
                prop_name_2: prop_val_2,
            },
            {
                db_id: 3,
                ...
            }
        ],
        icsd_id_2-icsd_id_3: [
            {
                db_id: 2,
                ...
            }
        ],
    },
    MP: {
        ...
        ...
    },
    ...
}

```

} ...

The rest of this document reports data curation performed on datasets generated via “Exact ICSD ID Matching” approach. For the analysis on the larger datasets generated by linking similar ICSD IDs using the structure matching method within MP, a similar curation approach was used.

D. Data Curation

1. Removing composition inconsistencies

From the ICSD UID to properties dictionary above, an ICSD UID key is removed if the entries within it do not have matching compositions. This process is done first within each of the three databases (discarded entries in Table IV), and then for UIDs common to pair-wise combinations of the databases (discarded entries in Table V). Most records filtered out at this step are materials with different number of H and Li atoms (e.g., BaGaH₄ vs BaGaH₅) or small changes in composition (e.g., Y₃Fe₂₉ vs Y₃Fe₃₁).

2. Filtering for the lowest energy entry per ICSD UID

For each ICSD UID, since there may exist multiple entries (calculations) in every database, only the entry with the lowest `total_energy_per_atom` value is retained from this step onward.

3. Removing records with unphysical properties

At this step, any records with unphysical values of certain properties are removed. This includes all boride formation energies from AFLOW, due to an error in the B chemical potential (this bug was discovered in the course of this work and confirmed by the AFLOW developers³³). Beyond AFLOW borides, unphysical properties are defined as per-atom formation energies outside -5 to $+5$ eV/atom, per-atom volumes above $150 \text{ \AA}^3/\text{atom}$, for all three databases (entries discarded at this step in Table VI).

4. Converting magnetizations into absolute values

Finally, all `total_magnetization_per_atom` values in all three databases are converted into absolute values.

When querying the Materials Project for total magnetization via the RESTful API, the value returned is not the total magnetic moment of the unit cell, as documented³⁴, but rather the per formula unit value. The magnetization values queried from Materials Project were normalized suitably.

Lastly, we identify the largest outliers for each property in each pairwise database comparison *post-curation*: formation energy in Table VII, volume in Table VIII, band gap in Table IX, and total magnetization in Table X.

Database Compositions		ICSD UID
AFLOW	Bi, YIO, Ba ₂ YCl ₇ , YBrO, Ba ₂ LaCl ₇ , Ba ₂ CeCl ₇ , AgSbTe ₂	0
AFLOW	LiB, Cr ₂ Te ₄ O ₁₁	1
AFLOW	BaGaH ₅ , BaGaH ₄	240693
AFLOW	SrGaH ₄ , SrGaH ₅	240697
OQMD	ZnCoCuAg, LiMgSnPd	16478

TABLE IV. Instances where composition did not match for records *within a database*.

TABLE V: Instances where composition did not match for records *across two databases being compared*.

Databases	Compositions	ICSD UID
AFLOW-MP	LiZnBi, ZnBi	100115
AFLOW-MP	Ba ₅ P ₃ HO ₁₃ , Ba ₅ P ₃ O ₁₃	62283
AFLOW-MP	RbOs ₂ HO ₉ , RbOs ₂ O ₉	20611
AFLOW-MP	Gd ₂ CBr ₂ , GdBr	47226
AFLOW-MP	Ba ₅ Cr ₃ HO ₁₃ , Ba ₅ Cr ₃ O ₁₃	21034
AFLOW-MP	YHO ₂ , YO ₂	28442
AFLOW-MP	SnPHO ₃ , SnPO ₃	25034
AFLOW-MP	Na ₃ VP ₂ HO ₉ , Na ₃ VP ₂ O ₉	50760
AFLOW-MP	Ta ₃ Al ₄ HO ₁₄ , Ta ₃ Al ₄ O ₁₄	67673
AFLOW-MP	Y ₃ Fe ₃₁ , Y ₃ Fe ₂₉	107259
AFLOW-MP	Ga(Bi ₄ O ₇) ₃ , Ga(Bi ₃ O ₅) ₄	68648
AFLOW-MP	NaCHO ₂ , NaCO ₂	109643
AFLOW-MP	KAl ₂ P ₂ H ₅ O ₁₁ , KAl ₂ P ₂ H ₄ O ₁₁	407355
AFLOW-MP	Rb ₃ H(SO ₄) ₂ , Rb ₃ (SO ₄) ₂	60050
AFLOW-MP	K ₂ Cr ₂ AsHO ₁₀ , K ₂ Cr ₂ AsO ₁₀	30533
AFLOW-MP	H ₂ O, H ₇ O ₄	27844
AFLOW-MP	Y ₁₂ (ReC ₃) ₅ , Y ₁₂ Re ₅ C ₆	658805
AFLOW-MP	Ba ₅ Re ₃ O ₁₇ , Ba ₅ Re ₃ O ₁₆	100777
AFLOW-MP	La ₃ TaH(O ₂ Cl) ₃ , La ₃ Ta(O ₂ Cl) ₃	62189
AFLOW-MP	CdHOCl, CdOCl	26752
AFLOW-MP	Tl ₃ HS ₂ O ₉ , Tl ₃ S ₂ O ₉	35358
AFLOW-MP	NdAl ₂ , Nd ₂ Al	608745
AFLOW-MP	LaNHO ₄ , LaNO ₄	413563
AFLOW-MP	C ₂ NHS ₂ (O ₂ F ₃) ₂ , C ₂ NS ₂ (O ₂ F ₃) ₂	50524
AFLOW-MP	XeSb ₂ F ₁₀ , Xe ₂ Sb ₄ F ₁₉	157664
AFLOW-MP	HO ₃ I, O ₃ I	26621
AFLOW-MP	NdMoHO ₁₅ I ₄ , NdMoO ₁₅ I ₄	281173
AFLOW-MP	Dy ₂ B ₃ HO ₈ , Dy ₂ B ₃ O ₈	413927
AFLOW-MP	LiCH ₃ O ₃ , LiCH ₂ O ₃	109604
AFLOW-MP	SrHF ₃ , SrF ₃	35408
AFLOW-MP	Li ₂ ScP ₂ HO ₈ , Li ₂ Sc(PO ₄) ₂	409955
AFLOW-MP	CaHOCl, CaOCl	24403
AFLOW-MP	CaCuAsHO ₅ , CaCuAsO ₅	64694
AFLOW-MP	BaAl ₅ HO ₉ , BaAl ₅ O ₉	33282
AFLOW-MP	Si ₂ N ₃ H, Si ₂ N ₃	202970
AFLOW-MP	RbHO, Rb ₂ O ₂	61048
AFLOW-MP	BaHF ₃ , BaF ₃	35409
AFLOW-MP	HoHO ₂ , HoO ₂	2944
AFLOW-MP	LiTa ₃ (Bi ₂ O ₇) ₂ , Ta ₃ (Bi ₂ O ₇) ₂	415141
AFLOW-MP	Ho ₂ B ₃ HO ₈ , Ho ₂ B ₃ O ₈	413928
AFLOW-MP	CdNHO ₄ , CdNO ₄	35355
AFLOW-MP	Na ₃ TiHF ₈ , Na ₃ TiF ₈	14131
AFLOW-MP	HgHO ₄ Cl, HgO ₄ Cl	29038
AFLOW-MP	SrNH, SrN	410656
AFLOW-MP	LaHO ₂ , LaO ₂	60675
AFLOW-MP	MnP ₂ HO ₇ , MnP ₂ O ₇	415152
AFLOW-OQMD	Y ₃ Fe ₃₁ , Y ₃ Fe ₂₉	107259
AFLOW-OQMD	Ga(Bi ₄ O ₇) ₃ , Ga(Bi ₃ O ₅) ₄	68648
AFLOW-OQMD	LiB, MnCoSiO ₄	2
AFLOW-OQMD	H ₂ O, H ₇ O ₄	27844
MP-OQMD	Bi ₃ (PO ₅) ₂ , SmPd	107679
MP-OQMD	BaGaH ₅ , BaGaH ₄	240693
MP-OQMD	SrGaH ₅ , SrGaH ₄	240697

Database	Composition	Property	value	ICSD	UID
Formation Energy (eV/atom)					
AFLOW	SiO ₂		-11.950	170547	
MP	Ta		5.113	54207	
OQMD	SiO ₂		84.972	155252	
OQMD	CuO ₂		1126.321	54126	
OQMD	Sc ₅ Ga ₃		8.575	165189	
Volume (Å ³ /atom)					
MP	HgH ₃ IO ₆		188.228	409499	
MP	HoVO ₄		364.707	152694	
MP	Na		349.842	70067	
MP	EuAg		962.227	58257	
MP	Ta		309.658	54207	
MP	Fe ₃ C		217.282	76827	
MP	Cu		603.475	150682	
MP	CaC ₂		896.388	252718	
MP	Rb		523.351	109016	
MP	TlCl ₂		386.012	20762	
MP	SnSe		182.422	52425	
MP	TcB		733.428	168896	
MP	K		433.990	157565	

TABLE VI. Records with physically unreasonable values of formation energy (outside the [−5, +5] eV/atom window) and/or volume (>150 Å³/atom).

Databases	Composition	ΔE_f^1 (eV/atom)	ΔE_f^2 (eV/atom)	Δ^{1-2}	ICSD	UID
AFLOW-MP	AlPO ₄	-2.780	-0.307	-2.474	162670	
AFLOW-MP	SiO ₂	-1.041	-2.870	1.829	25632	
AFLOW-MP	O	0.004	1.669	-1.665	92775	
AFLOW-MP	AlClO	-1.741	-2.789	1.048	27812	
AFLOW-MP	Bi	0.135	1.090	-0.954	51675	
AFLOW-MP	YAl ₃	0.515	-0.437	0.952	58220	
AFLOW-MP	PCl ₅	-0.192	-1.061	0.869	76731	
AFLOW-MP	K ₂ BeO ₂	-1.259	-2.124	0.865	23633	
AFLOW-MP	Li ₄ P ₂ O ₇	-1.899	-2.762	0.863	39814	
AFLOW-MP	RbC ₈	0.751	-0.030	0.781	200563	
AFLOW-OQMD						
AFLOW-OQMD	AlPO ₄	-2.780	-0.237	-2.543	162670	
AFLOW-OQMD	O	0.004	1.395	-1.391	92775	
AFLOW-OQMD	MgO	-2.877	-1.879	-0.998	181459	
AFLOW-OQMD	AlClO	-1.741	-2.608	0.867	27812	
AFLOW-OQMD	RbC ₈	0.751	-0.040	0.791	200563	
AFLOW-OQMD	K ₂ BeO ₂	-1.259	-2.002	0.743	23633	
AFLOW-OQMD	SrPSe ₃	-0.277	-1.016	0.739	412766	
AFLOW-OQMD	Li ₄ P ₂ O ₇	-1.899	-2.634	0.735	39814	
AFLOW-OQMD	PCl ₅	-0.192	-0.908	0.716	76731	
AFLOW-OQMD	Mg ₃ P ₂ O ₈	-2.346	-2.930	0.584	9849	
MP-OQMD						
MP-OQMD	MnNiAs	3.547	-0.249	3.796	161716	
MP-OQMD	Nd ₃ PbN	-0.945	1.319	-2.264	76397	
MP-OQMD	IrC ₄	0.981	3.161	-2.180	181498	
MP-OQMD	Nd ₃ SnN	-1.029	1.112	-2.141	76398	
MP-OQMD	Sm ₃ AlN	-0.894	1.109	-2.003	52640	
MP-OQMD	LiNO ₃	0.690	-1.252	1.942	33661	
MP-OQMD	Pr ₃ AlN	-0.788	1.101	-1.888	52639	
MP-OQMD	Cr ₃ O	1.971	0.141	1.830	15904	
MP-OQMD	Eu(Cu ₂ Sn) ₂	1.296	-0.322	1.617	416796	
MP-OQMD	GdMg ₂ Ag	1.502	-0.102	1.605	107733	

TABLE VII. Top ten outliers in calculated formation energy across pairwise comparisons of databases.

Databases	Composition	V^1	V^2	Δ^{1-2}	ICSD UID
		(Å ³ /atom)			
AFLOW-MP	Bi	31.51	103.72	-72.21	51675
AFLOW-MP	MnNiAs	15.70	84.29	-68.59	161716
AFLOW-MP	Hg	28.86	95.21	-66.35	79804
AFLOW-MP	HoS	39.85	103.31	-63.46	66357
AFLOW-MP	SrPSe ₃	89.79	27.94	61.85	412766
AFLOW-MP	NbTeBr ₃	75.01	34.02	40.99	35376
AFLOW-MP	CeBr ₃	67.72	31.52	36.20	31582
AFLOW-MP	Se	63.04	31.90	31.14	150731
AFLOW-MP	FeSeBr ₇	66.74	37.16	29.58	39528
AFLOW-MP	SnSe	27.09	56.42	-29.34	71338
AFLOW-OQMD	SrPSe ₃	89.79	27.65	62.14	412766
AFLOW-OQMD	NbTeBr ₃	75.01	30.71	44.30	35376
AFLOW-OQMD	CeBr ₃	67.72	31.01	36.71	31582
AFLOW-OQMD	H	37.20	2.73	34.47	28465
AFLOW-OQMD	CsTl	14.22	47.71	-33.49	165344
AFLOW-OQMD	Se	63.04	31.39	31.65	150731
AFLOW-OQMD	FeSeBr ₇	66.74	37.22	29.52	39528
AFLOW-OQMD	CaPSe ₃	53.48	25.50	27.98	412765
AFLOW-OQMD	SnSe	27.09	52.60	-25.52	71338
AFLOW-OQMD	TiO ₂	35.12	11.39	23.73	97008
MP-OQMD	Bi	103.72	31.53	72.20	51675
MP-OQMD	MnNiAs	84.29	14.74	69.55	161716
MP-OQMD	Hg	95.21	27.10	68.11	79804
MP-OQMD	CoO ₂	57.55	11.71	45.84	89837
MP-OQMD	H ₂	43.46	5.38	38.07	28344
MP-OQMD	Cd ₆ Sb ₅	62.94	31.30	31.65	52832
MP-OQMD	Cl ₂	70.98	41.47	29.50	22406
MP-OQMD	LiBH ₄	37.31	9.87	27.44	168803
MP-OQMD	HfPd ₅	41.53	15.69	25.84	168289
MP-OQMD	Xe	83.51	58.86	24.65	9786

TABLE VIII. Top ten outliers in calculated volume across pairwise comparisons of databases.

Databases	Composition	E_g^1	E_g^2	Δ^{1-2}	ICSD	UID
		(eV)				
AFLOW-MP	CeF ₃	5.87	0.00	5.87	42470	
AFLOW-MP	LiAlPHO ₅	0.02	5.72	-5.70	68921	
AFLOW-MP	Na ₂ PHO ₃	0.00	5.58	-5.58	155976	
AFLOW-MP	KCeF ₄	5.44	0.00	5.44	23229	
AFLOW-MP	RbYbF ₃	1.09	6.52	-5.43	49590	
AFLOW-MP	K ₅ NaCe ₂ S ₆ O ₂₄	5.49	0.08	5.41	281576	
AFLOW-MP	CsYbF ₃	1.78	7.05	-5.26	49579	
AFLOW-MP	BaTm ₂ F ₈	1.97	7.24	-5.26	20103	
AFLOW-MP	CePO ₄	5.23	0.00	5.23	184550	
AFLOW-MP	Mg ₃ P ₂ O ₈	0.00	5.18	-5.18	9849	
AFLOW-OQMD	BeF ₂	8.04	0.00	8.04	173557	
AFLOW-OQMD	KYb ₃ F ₁₀	0.97	8.44	-7.47	28258	
AFLOW-OQMD	NaCaAlF ₆	7.12	0.00	7.12	80542	
AFLOW-OQMD	H ₂₄ OsC ₈ N ₂ F ₆	0.00	6.68	-6.68	151185	
AFLOW-OQMD	YbCl ₃ O ₁₂	0.00	6.38	-6.38	85762	
AFLOW-OQMD	LiAlPHO ₅	0.02	6.20	-6.18	68921	
AFLOW-OQMD	LiEuP ₄ O ₁₂	0.33	6.41	-6.08	416878	
AFLOW-OQMD	Na ₂ PHO ₃	0.00	6.07	-6.07	155976	
AFLOW-OQMD	CoSiH ₁₂ O ₆ F ₆	0.00	5.96	-5.96	2900	
AFLOW-OQMD	CsYbF ₃	1.78	7.73	-5.94	49579	
MP-OQMD	KYb ₃ F ₁₀	0.00	8.44	-8.44	28258	
MP-OQMD	BeF ₂	7.96	0.00	7.96	173557	
MP-OQMD	KCeF ₄	0.00	7.75	-7.75	23229	
MP-OQMD	H ₂	0.00	7.22	-7.22	28539	
MP-OQMD	NaCaAlF ₆	7.11	0.00	7.11	80542	
MP-OQMD	EuMgF ₄	0.29	7.22	-6.94	86246	
MP-OQMD	CsEuF ₃	0.00	6.93	-6.93	49577	
MP-OQMD	H ₂₄ OsC ₈ (NF ₃) ₂	0.17	6.68	-6.51	151185	
MP-OQMD	Yb(ClO ₄) ₃	0.00	6.46	-6.46	85763	
MP-OQMD	LiEu(PO ₃) ₄	0.00	6.41	-6.41	416878	

TABLE IX. Top ten outliers in calculated band gap across pairwise comparisons of databases.

Databases	Composition	M^1	M^2	Δ^{1-2}	ICSD	UID
		(μ_B /atom)				
AFLOW-MP	YbMn ₂₈	124.89	7.16	117.72	643923	
AFLOW-MP	Pr ₆ Mn ₂₃	121.85	32.42	89.43	643337	
AFLOW-MP	BaMn ₂₈	87.51	8.61	78.90	615966	
AFLOW-MP	Yb ₆ Mn ₂₃	105.23	29.18	76.05	643920	
AFLOW-MP	Ba ₆ Co ₂₅ S ₂₇	66.99	0.00	66.99	71939	
AFLOW-MP	Mn ₂₀ W ₃ C ₆	74.10	16.64	57.46	618279	
AFLOW-MP	Mn ₂₀ Mo ₃ C ₆	73.37	16.53	56.84	618260	
AFLOW-MP	Gd ₈ Rh ₅ C ₁₂	56.95	0.15	56.80	617956	
AFLOW-MP	Nd ₁₂ Co ₆ Sn	56.33	0.00	56.33	240094	
AFLOW-MP	Yb ₆ Co ₃₀ P ₁₉	56.51	1.12	55.39	67950	
AFLOW-OQMD	EuMn ₂₈	125.94	4.13	121.82	631390	
AFLOW-OQMD	Gd ₁₃ Ge ₆ O ₃₁ F	90.97	0.01	90.96	62329	
AFLOW-OQMD	Pr ₆ Mn ₂₃	121.85	33.03	88.82	643337	
AFLOW-OQMD	BaMn ₂₈	87.51	5.58	81.93	615966	
AFLOW-OQMD	Yb ₆ Mn ₂₃	105.23	30.78	74.45	643920	
AFLOW-OQMD	Ba ₆ Co ₂₅ S ₂₇	66.99	2.23	64.76	71939	
AFLOW-OQMD	Nd ₁₂ Co ₆ Sn	56.33	0.01	56.32	240094	
AFLOW-OQMD	Gd ₇ Pd ₃	54.76	0.89	53.86	104112	
AFLOW-OQMD	Gd ₇ CoI ₁₂	51.02	0.00	51.01	245279	
AFLOW-OQMD	ThMn ₁₂	52.10	2.25	49.86	104986	
MP-OQMD	Gd ₁₃ Ge ₆ O ₃₁ F	91.00	0.01	90.99	62329	
MP-OQMD	ZnFe ₁₆ Ni ₇ O ₃₂	38.00	94.00	-56.00	182238	
MP-OQMD	Eu ₇ Au ₃	50.72	0.01	50.71	611842	
MP-OQMD	Gd ₆ Zn ₂₃	42.88	0.01	42.87	636504	
MP-OQMD	Gd ₆ C ₃ Cl ₅	42.69	0.00	42.68	202547	
MP-OQMD	Gd ₁₀ S ₁₉	42.00	0.00	42.00	416804	
MP-OQMD	Ba ₈ Eu ₇ Cl ₃₄	45.00	4.02	40.98	408479	
MP-OQMD	Mn ₉ Au ₃₁	0.28	39.05	-38.77	58552	
MP-OQMD	Eu ₅ Pd ₂	36.02	0.00	36.02	631525	
MP-OQMD	Eu ₅ Pt ₂	35.94	0.00	35.94	631557	

TABLE X. Top ten outliers in calculated total magnetization across pairwise comparisons of databases.

III. PER-MATERIAL-CLASS MEDIAN ABSOLUTE DIFFERENCES

	AFLOW vs MP				AFLOW vs OQMD				MP vs OQMD			
	ΔE_f	V	E_g	M	ΔE_f	V	E_g	M	ΔE_f	V	E_g	M
All	0.105 (207)	0.180 (19258)	0.078 (10063)	0.015 (4125)	0.019 (1717)	0.647 (15857)	0.209 (8044)	0.149 (2951)	0.087 (19082)	0.512 (19082)	0.178 (9914)	0.012 (3770)
Oxide	0.160 (989)	0.091 (6468)	0.088 (5289)	0.002 (1694)	0.020 (818)	0.820 (5269)	0.252 (4208)	0.003 (1159)	0.161 (6616)	0.787 (6616)	0.248 (5300)	0.001 (1601)
Nitride	0 (0)	0.174 (1639)	0.057 (1193)	0.006 (218)	0 (0)	1.254 (1257)	0.222 (936)	0.363 (149)	0.115 (1422)	1.030 (1422)	0.180 (1068)	0.013 (199)
Pnictide	0.106 (727)	0.161 (5470)	0.056 (3520)	0.008 (919)	0.026 (611)	0.721 (4330)	0.193 (2735)	0.067 (554)	0.106 (5210)	0.639 (5210)	0.178 (3385)	0.009 (805)
Chalcogenide	0.022 (412)	0.244 (3985)	0.077 (2982)	0.004 (714)	0.019 (340)	0.768 (3154)	0.153 (2328)	0.028 (470)	0.153 (3951)	0.592 (3951)	0.134 (2924)	0.006 (623)
Halide	0.208 (298)	0.200 (3850)	0.073 (3291)	0.001 (891)	0.125 (245)	1.648 (3107)	0.221 (2565)	0.002 (567)	0.125 (3700)	1.478 (3700)	0.164 (3029)	0.001 (725)
Alkali Metal	0.096 (695)	0.131 (4541)	0.064 (3605)	0.001 (897)	0.018 (599)	0.912 (3887)	0.231 (3019)	0.002 (618)	0.112 (4961)	0.877 (4961)	0.201 (3904)	0 (860)
Alkaline Earth Metal	0.088 (709)	0.088 (3446)	0.039 (2002)	0.003 (621)	0.014 (580)	0.527 (2928)	0.213 (1614)	0.010 (466)	0.095 (3398)	0.507 (3398)	0.205 (1960)	0.003 (575)
Transition Metal	0.066 (393)	0.206 (13028)	0.181 (5342)	0.025 (3595)	0.018 (313)	0.574 (10669)	0.203 (4176)	0.158 (2773)	0.065 (12500)	0.404 (12500)	0.157 (5025)	0.010 (3447)
Metalloid	0.106 (1063)	0.154 (6004)	0.040 (2965)	0.166 (979)	0.018 (856)	0.465 (4926)	0.187 (2330)	0.811 (637)	0.032 (5933)	0.342 (5933)	0.184 (2879)	0.037 (766)
Rare-Earth	0.013 (63)	0.207 (4630)	0.152 (1236)	0.173 (1229)	0.005 (48)	0.387 (3974)	0.222 (1038)	2.637 (651)	0.048 (5511)	0.285 (5511)	0.197 (1610)	0.144 (977)
Actinide	0.096 (4)	0.585 (670)	0.851 (222)	0.265 (300)	0.110 (4)	1.027 (569)	0.278 (187)	0.273 (272)	0.074 (758)	0.250 (758)	1.019 (233)	0.054 (438)
Metal-Nonmetal	0.138 (1246)	0.143 (12270)	0.095 (6717)	0.002 (3053)	0.021 (1035)	0.790 (10020)	0.218 (7004)	0.004 (2129)	0.135 (12374)	0.688 (12374)	0.185 (6890)	0.002 (2829)
Intermetallic	0.009 (182)	0.300 (3056)	0.066 (50)	1.163 (528)	0.005 (157)	0.319 (2982)	0.213 (35)	1.712 (404)	0.011 (2910)	0.238 (2910)	0.176 (54)	0.182 (446)
Magnetic	0.025 (12)	0.250 (4125)	0.462 (1580)	0.015 (4125)	0.222 (5)	0.900 (2951)	0.402 (1013)	0.149 (2951)	0.093 (3770)	0.495 (3770)	0.202 (1330)	0.012 (3770)
Non-Magnetic	0.108 (1991)	0.160 (13119)	0.051 (8106)	0 (0)	0.019 (1680)	0.609 (10520)	0.185 (6522)	0 (0)	0.087 (12922)	0.527 (12922)	0.169 (8146)	0 (0)
Disagree On Magnetic	0.020 (67)	0.234 (2014)	0.330 (377)	0 (0)	0.007 (32)	0.489 (2386)	0.402 (509)	0 (0)	0.079 (2390)	0.483 (2390)	0.752 (438)	0 (0)
Metallic	0.007 (498)	0.236 (7951)	0 (0)	0.733 (1888)	0.004 (436)	0.320 (6769)	0 (0)	1.571 (158)	0.014 (8002)	0.194 (8002)	0 (0)	0.090 (2066)
Semiconductor	0.032 (472)	0.162 (2456)	0.084 (2456)	0.002 (394)	0.020 (328)	0.514 (1743)	0.139 (1743)	0.002 (231)	0.091 (2400)	0.508 (2400)	0.126 (2400)	0.001 (445)
Insulator	0.159 (1032)	0.108 (6785)	0.056 (6785)	0 (751)	0.021 (855)	0.999 (5577)	0.216 (5577)	0.001 (500)	0.152 (6791)	0.953 (6791)	0.193 (6791)	0 (656)
Disagree On Metallic	0.022 (47)	0.274 (1239)	0 (0)	0.006 (566)	0.016 (32)	0.928 (981)	0 (0)	0.009 (419)	0.115 (1001)	0.674 (1001)	0 (0)	0.003 (361)
Pseudopotentials Agree	0.116 (1547)	0.165 (11410)	0.071 (6621)	0.005 (2571)	0.022 (1139)	0.819 (5639)	0.173 (3793)	0.037 (453)	0.103 (10616)	0.599 (6604)	0.176 (990)	0.026 (2026)
Pseudopotentials Disagree	0.068 (523)	0.198 (7848)	0.093 (3442)	0.143 (1554)	0.011 (578)	0.576 (10222)	0.245 (4251)	0.211 (2498)	0.073 (8466)	0.429 (8466)	0.184 (3310)	0.008 (2790)
Element	0.007 (91)	0.409 (159)	0.068 (45)	0.216 (8)	0.004 (76)	0.755 (149)	0.212 (33)	0.392 (5)	0.007 (152)	0.523 (152)	0.151 (42)	0.032 (6)
Binary	0.032 (648)	0.279 (3932)	0.048 (875)	0.338 (492)	0.024 (542)	0.508 (2698)	0.177 (790)	0.819 (377)	0.027 (2934)	0.330 (2934)	0.141 (877)	0.073 (438)
Ternary	0.103 (1003)	0.193 (10319)	0.067 (4526)	0.155 (2229)	0.020 (841)	0.518 (8706)	0.192 (3720)	0.671 (1665)	0.059 (10423)	0.371 (10423)	0.162 (4443)	0.030 (2025)
Quaternary	0.158 (308)	0.114 (4270)	0.098 (3530)	0.002 (1130)	0.015 (250)	0.819 (3438)	0.223 (2786)	0.003 (725)	0.150 (4497)	0.748 (4497)	0.204 (3630)	0.002 (1022)
Triclinic	0.150 (104)	0.147 (1003)	0.089 (902)	0.002 (216)	0.021 (89)	1.165 (805)	0.202 (714)	0.002 (132)	0.156 (1052)	1.053 (1052)	0.204 (930)	0 (207)
Monoclinic	0.134 (446)	0.170 (3691)	0.086 (2991)	0.002 (764)	0.026 (373)	0.969 (2991)	0.211 (2340)	0.003 (491)	0.138 (4052)	0.828 (4052)	0.178 (3178)	0.001 (738)
Orthorhombic	0.103 (507)	0.169 (4550)	0.072 (2552)	0.008 (746)	0.020 (405)	0.599 (3629)	0.190 (1953)	0.054 (522)	0.078 (4634)	0.487 (4634)	0.163 (2509)	0.010 (724)
Tetragonal	0.090 (246)	0.196 (2797)	0.090 (1042)	0.190 (641)	0.020 (202)	0.521 (2369)	0.216 (861)	0.897 (496)	0.050 (2762)	0.382 (2762)	0.174 (980)	0.052 (572)
Trigonal	0.099 (241)	0.162 (1746)	0.072 (1144)	0.002 (389)	0.016 (199)	0.634 (1404)	0.240 (896)	0.003 (285)	0.117 (1507)	0.549 (1507)	0.181 (947)	0.002 (326)
Hexagonal	0.032 (198)	0.187 (2108)	0.055 (545)	0.252 (427)	0.008 (158)	0.372 (1626)	0.190 (438)	0.767 (231)	0.024 (1798)	0.255 (1798)	0.200 (440)	0.065 (338)
Cubic	0.040 (295)	0.197 (2988)	0.064 (752)	0.540 (795)	0.015 (217)	0.436 (2203)	0.213 (527)	0.972 (541)	0.027 (2343)	0.268 (2343)	0.189 (600)	0.052 (557)

FIG. S 1. Median absolute differences between properties (formation energy, volume, band gap, total magnetization) are in units of eV/atom, Å³/atom, eV, and μ_B /formula unit, respectively) calculated in the three databases (AFLOW, MP, OQMD), compared pairwise, across various classes of materials as defined in Table III of the main text. The numbers in parentheses indicate the number of overlapping records belonging to the respective material class for a given pair of databases. Trivial comparisons are left blank (e.g., the difference in total magnetization for non-magnetic compounds).

IV. ELEMENT-WISE ANALYSIS OF HT-DFT DIFFERENCES

To study the source of differences between the various HT-DFT databases, we collect statistics for the four properties being compared—formation energy, volume, band gap, total magnetization—averaged over all records containing a certain element in the periodic table. For each element, we also present the pseudopotential (psp) used in the two databases being compared, and the number of comparable records of compounds containing the element over which statistical quantities are computed.

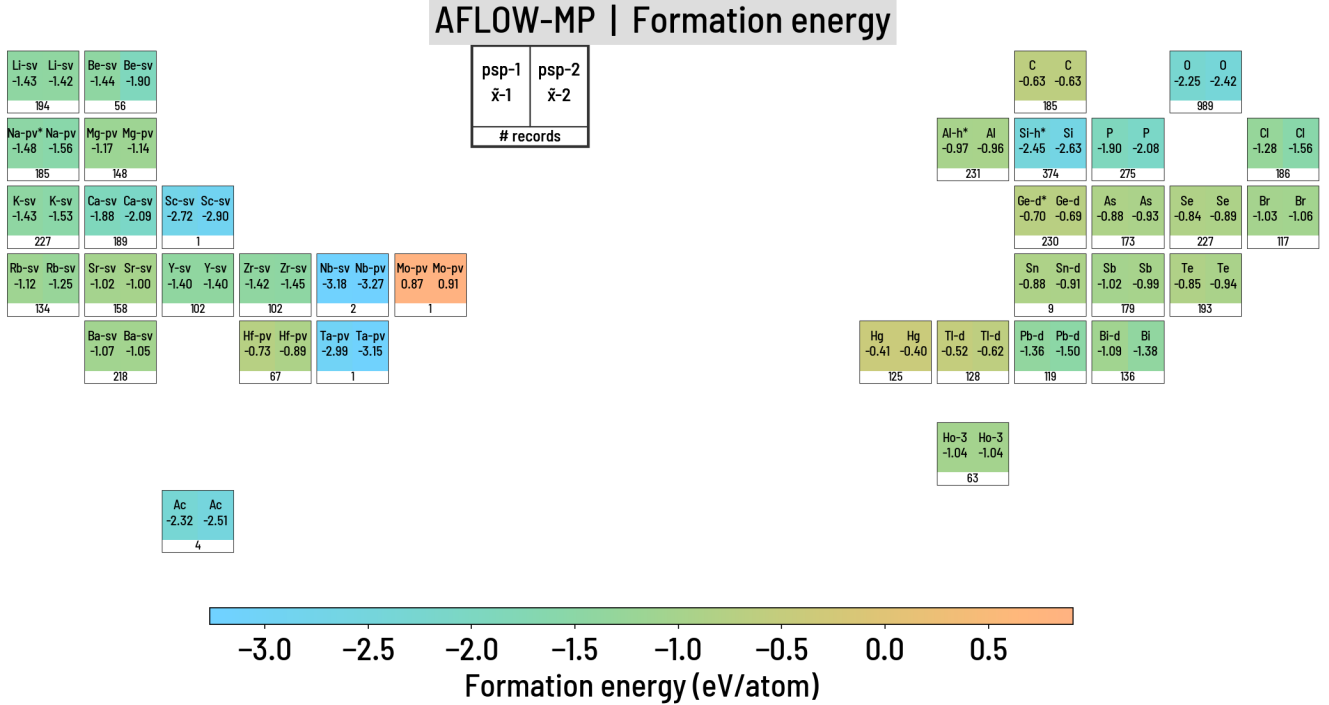


FIG. S2. Median values of formation energy for compounds containing a certain element in the periodic table, for a comparison of AFLOW and MP. The VASP PAW potential used for each element and the number of records in each comparison are indicated (* indicates more than one pseudopotential used in the database overall for that element).

AFLOW-MP | Volume

H H				DB-1 DB-2																		
Li-sv	Li-sv	Be-sv	Be-sv	psp-1	psp-2			B*	B	C	C	N	N	O	O	F	F					
11.73	11.63	12.03	12.06			1045		12.04	11.86	14.44	14.15	14.37	14.11	14.34	14.23	15.69	15.53					
1660		1010	203							1555		1639		6468								
Li-sv Na-pv	Na-pv	Mg-pv	Mg-pv			Al-h*	Al	Si-h*	Si	P	P	S	S	Cl	Cl							
13.82	13.80	16.41	16.52			1101		16.34	16.28	15.23	15.06	21.80	21.50									
999		601				1477		16.88		1813		2011										
K-sv K-sv	Ca-sv Ca-sv	Sc-sv Sc-sv	Ti-sv Ti-pv	V-sv V-pv	Cr-pv Cr-pv	Mn-pv Mn-pv	Fe-pv Fe-pv	Co Co	Ni-pv Ni-pv	Cu-pv Cu-pv	Zn Zn	Ga-h Ga-d	Ge-d* Ge-d	As As	Se Se	Br Br						
18.40	18.40	15.74	15.56	14.41	14.30	15.12	14.40	15.36	14.76	16.68	16.46	17.33	17.62	18.45	18.48	19.89	18.70	25.06	24.71	29.99	29.78	
14.28		783	379	539	577	433	659	776	1028	1226	726	658	1094	863								
Rb-sv Rb-sv	Sr-sv Sr-sv	Y-sv Y-sv	Zr-sv Zr-sv	Nb-sv Nb-pv	Mo-pv Mo-pv	Tc-pv Tc-pv	Ru-pv Ru-pv	Rh-pv Rh-pv	Pd-pv Pd	Ag Ag	Cd Cd	In-d In-d	Sn Sn-d	Sb Sb	Te Te	I I						
21.87	21.83	17.00	16.91	18.52	18.64	17.15	17.12	16.88	16.61	16.10	16.00	19.69	19.78	21.21	20.86	23.21	22.73	23.64	23.26	27.77	27.45	
818		815	544	501	473	535	72	366	497	675	647	585	732	882	870							
Cs* Cs-sv	Ba-sv Ba-sv	Lu-3* Lu-3	Hf-pv Hf-pv	Ta-pv Ta-pv	W-pv W-pv	Re-pv Re-pv	Os-pv Os-pv	Ir Ir	Pt Pt	Au Au	Hg Hg	Tl-d Tl-d	Pb-d Pb-d	Bi-d Bi								
27.25	27.12	18.39	18.22	18.77	18.95	17.23	17.09	15.51	15.34	14.78	14.66	292	236	420	602	595	394	554	505	540		
618		1205	120	307	401	315																

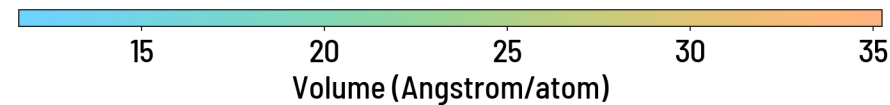


FIG. S3. Median values of per-atom volume for compounds containing a certain element in the periodic table, for a comparison of AFLOW and MP. The VASP PAW potential used for each element and the number of records in each comparison are indicated (* indicates more than one pseudopotential used in the database overall for that element).

AFLOW-MP | Band gap

H H				DB-1 DB-2																				
Li-sv	Li-sv	Be-sv	Be-sv	psp-1	psp-2			B*	B	C	C	N	N	O	O	F	F							
3.08	3.06	4.38	4.43			488		3.91	3.81	3.26	3.10	2.78	2.69	2.97	2.87	3.70	3.71							
654		143				402		2.71	2.71	2.04	2.07	2.08	2.09	2.09	2.07	3.56	3.63	443	426	470	44			
Na-pv* Na-pv	Na-pv	Mg-pv	Mg-pv			358		2.51	2.51	2.04	2.07	1.75	1.75	1.75	1.75	1.71	1.72	1.73	1.73	1.73	1.73	1.73		
2.95	2.78	3.56	3.57			817				2	81	246				457	443	426	470	44	373			
817		289																						
K-sv K-sv	Ca-sv Ca-sv	Sc-sv Sc-sv	Ti-sv Ti-pv	V-sv V-pv	Cr-pv Cr-pv	Mn-pv Mn-pv	Fe-pv Fe-pv	Co Co	Ni-pv Ni-pv	Cu-pv Cu-pv	Zn Zn	Ga-h Ga-d	Ge-d* Ge-d	As As	Se Se	Br Br								
2.45	2.29	3.27	3.26	3.05	3.41	2.71	2.10	2.19	2.20	2.16	319	269	190	180	472	408	246	387	526	1.74	1.74			
1212		459	120	209	352	352										444	678	1257	1583	1094				
Rb-sv Rb-sv	Sr-sv Sr-sv	Y-sv Y-sv	Zr-sv Zr-sv	Nb-sv Nb-pv	Mo-pv Mo-pv	Tc-pv Tc-pv	Ru-pv Ru-pv	Rh-pv Rh-pv	Pd-pv Pd	Ag Ag	Cd Cd	In-d In-d	Sn Sn-d	Sb Sb	Te Te	I I								
2.34	2.17	2.53	2.31	3.00	2.90	2.71	3.10	1.89	1.75	2.44	2.55	27	62	43	150	390	345	245	322	453	583	529		
684		480	199	187	211	318										444	678	1257	1583	1094				
Cs* Cs-sv	Ba-sv Ba-sv	Lu-3* Lu-3	Hf-pv Hf-pv	Ta-pv Ta-pv	W-pv W-pv	Re-pv Re-pv	Os-pv Os-pv	Ir Ir	Pt Pt	Au Au	Hg Hg	Tl-d Tl-d	Pb-d Pb-d	Bi-d Bi										
2.38	2.21	2.34	2.21	2.01	2.17	2.83	2.81	2.78	2.67	2.39	2.46	110	53	34	130	771	266	345	300	324				
526		751	27	79	200	178										260	62	118	116	117	139	34		
La La	La La	Ce Ce	Pr Pr	Nd Nd	Pm* Pm-3	Sm-3* Sm-3	Eu Eu									Tb-3 Tb-3	Dy-3 Dy-3	Ho-3 Ho-3	Er-3 Er-3	Tm Tm-3	Yb-2* Yb-2			
2.37	2.29	2.23	0.26	2.89	3.10	3.71	0.43	0.43	1.91	2.14	0.56					2.21	2.21	1.98	1.89	1.81	1.97	1.92		
260		62	82	4	142	1	5	48								112	116	117	139	4	34			
Ac Ac	Th-s Th	Pa Pa	U U	Pa Pa	U U																			
4.11	4.10	2.74	2.71	2.16	2.19	2.87	1.85	1.85	1.85	1.85	1.85													
3		69	4	142																				



FIG. S4. Median values of band gap for compounds containing a certain element in the periodic table, for a comparison of AFLOW and MP. The VASP PAW potential used for each element and the number of records in each comparison are indicated (* indicates more than one pseudopotential used in the database overall for that element).

AFLOW-MP | Total magnetization

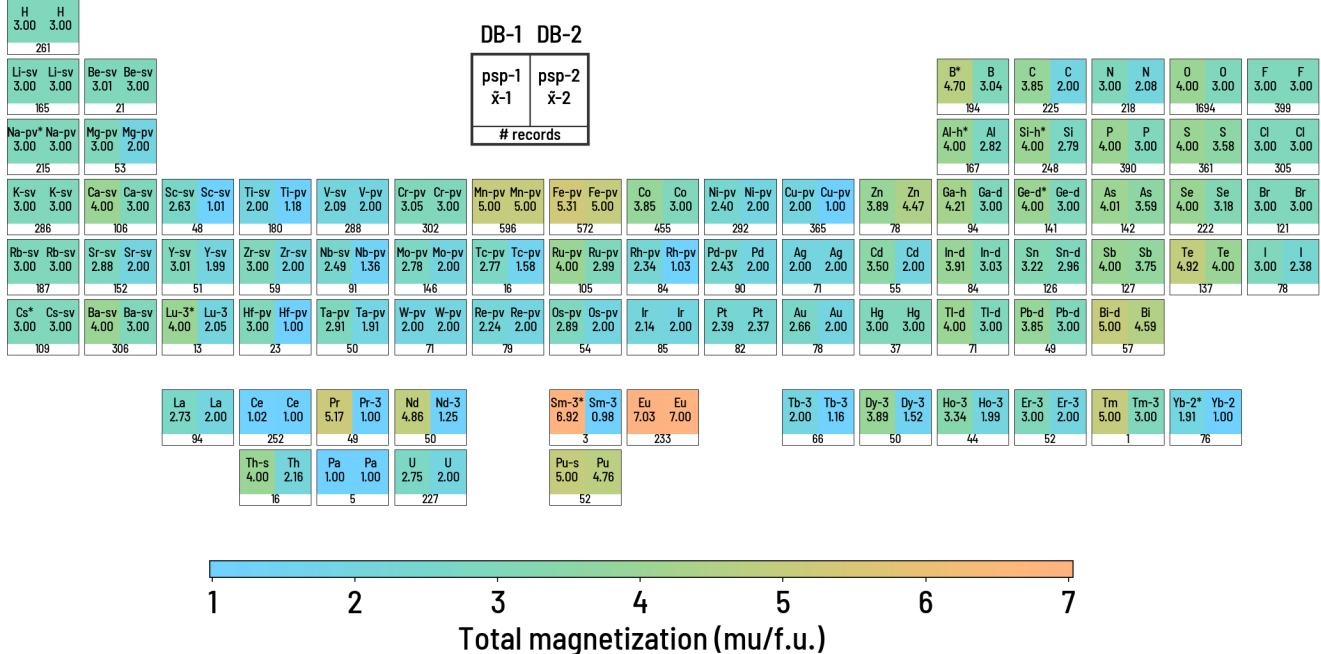


FIG. S5. Median values of total magnetization (per formula unit) for compounds containing a certain element in the periodic table, for a comparison of AFLOW and MP. The VASP PAW potential used for each element and the number of records in each comparison (* indicates more than one pseudopotential used in the database overall for that element).

AFLOW-OQMD | Formation energy

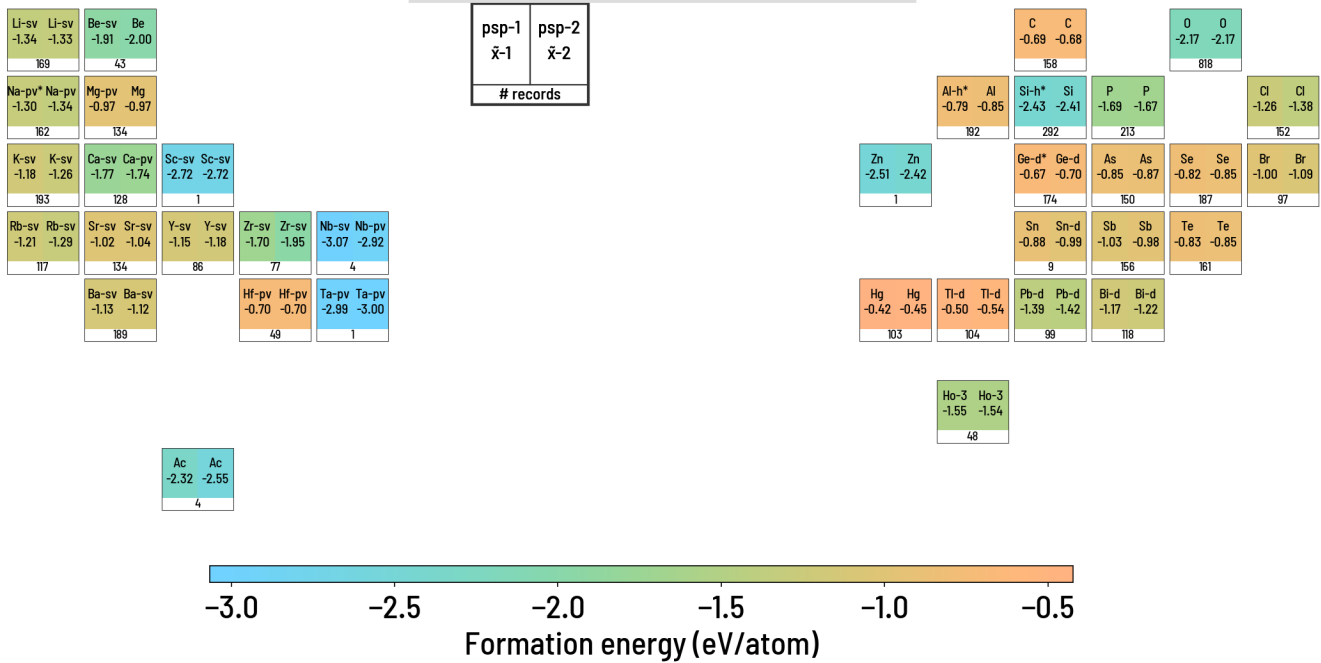


FIG. S6. Median values of formation energy for compounds containing a certain element in the periodic table, for a comparison of AFLow and OQMD. The VASP PAW potential used for each element and the number of records in each comparison (* indicates more than one pseudopotential used in the database overall for that element).

AFLOW-OQMD | Volume

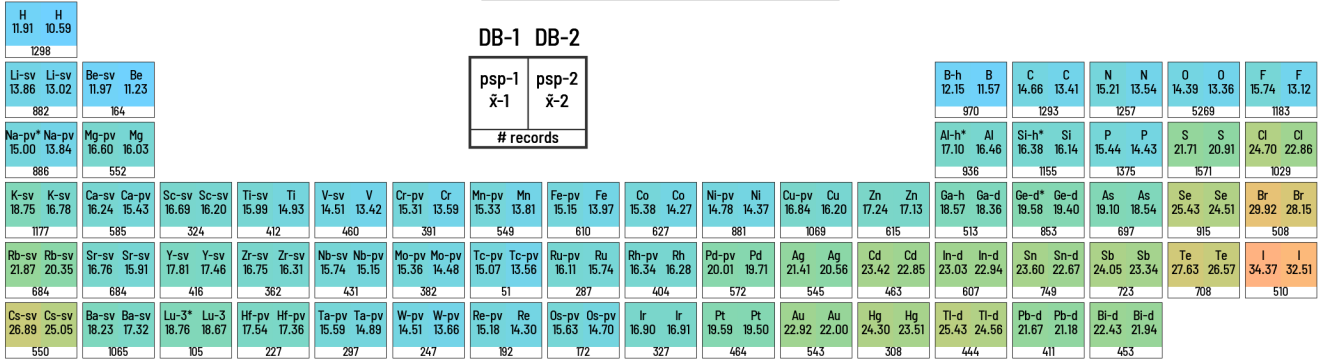


FIG. S7. Median values of per-atom volume for compounds containing a certain element in the periodic table, for a comparison of AFLOW and OQMD. The VASP PAW potential used for each element and the number of records in each comparison are indicated (* indicates more than one pseudopotential used in the database overall for that element).

AFLOW-OQMD | Band gap

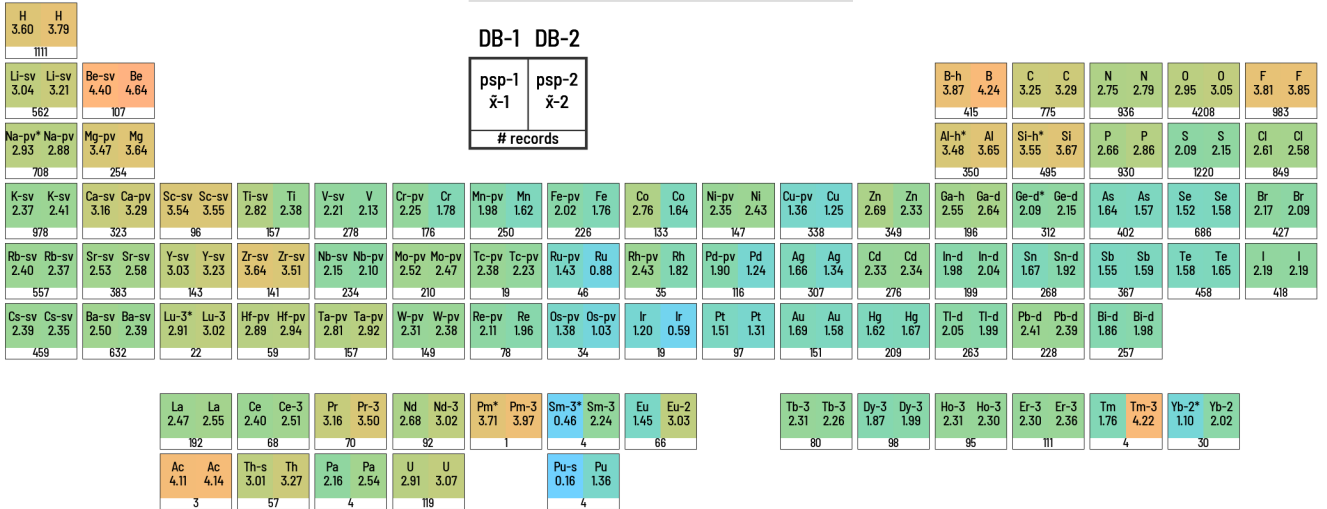


FIG. S8. Median values of band gap for compounds containing a certain element in the periodic table, for a comparison of AFLOW and OQMD. The VASP PAW potential used for each element and the number of records in each comparison are indicated (* indicates more than one pseudopotential used in the database overall for that element).

AFLOW-OQMD | Total magnetization

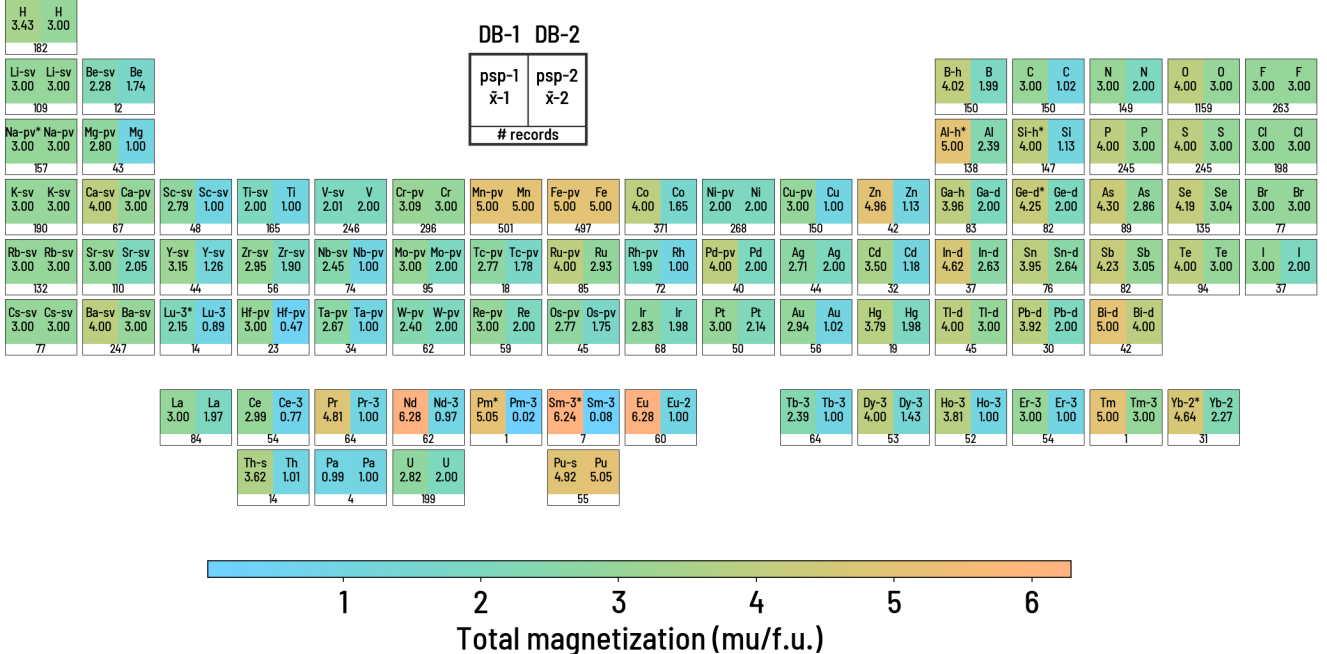


FIG. S 9. Median values of total magnetization (per formula unit) for compounds containing a certain element in the periodic table, for a comparison of AFLOW and OQMD. The VASP PAW potential used for each element and the number of records in each comparison are indicated (* indicates more than one pseudopotential used in the database overall for that element).

MP-OQMD | Formation energy

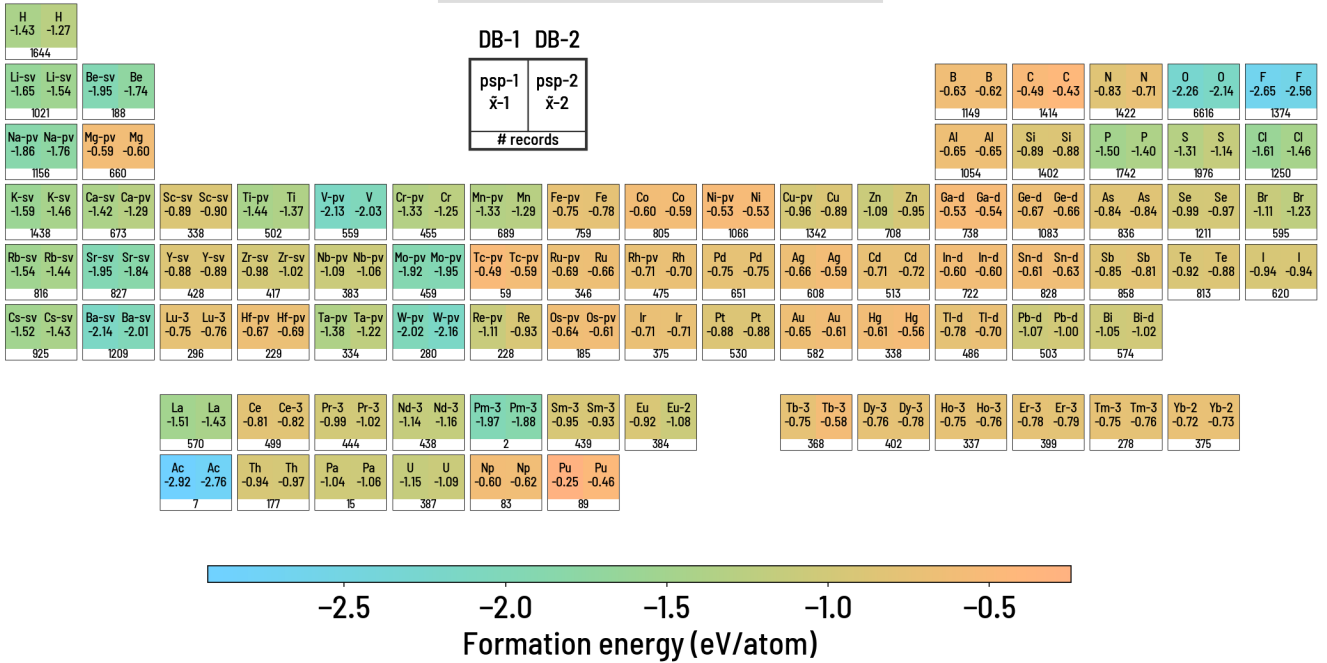


FIG. S 10. Median values of formation energy for compounds containing a certain element in the periodic table, for a comparison of MP and OQMD. The VASP PAW potential used for each element and the number of records in each comparison are indicated (* indicates more than one pseudopotential used in the database overall for that element).

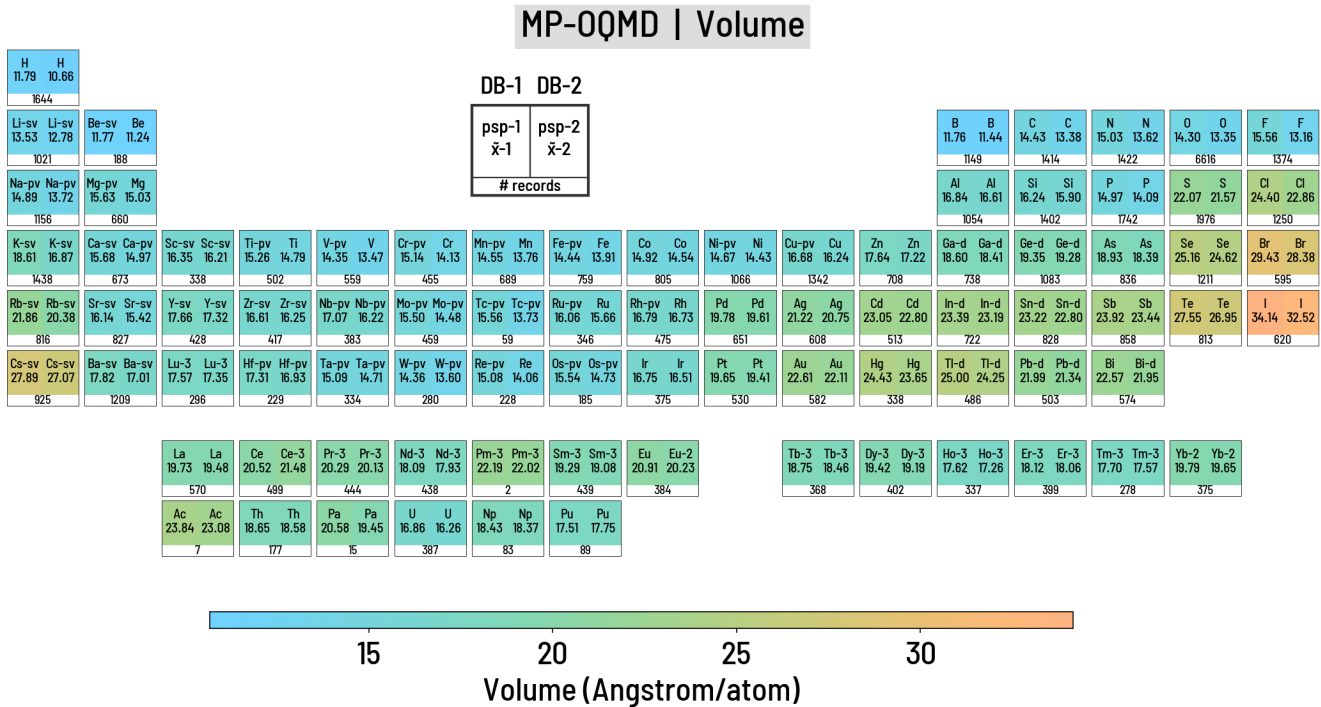


FIG. S11. Median values of per-atom volume for compounds containing a certain element in the periodic table, for a comparison of MP and OQMD. The VASP PAW potential used for each element and the number of records in each comparison are indicated (* indicates more than one pseudopotential used in the database overall for that element).

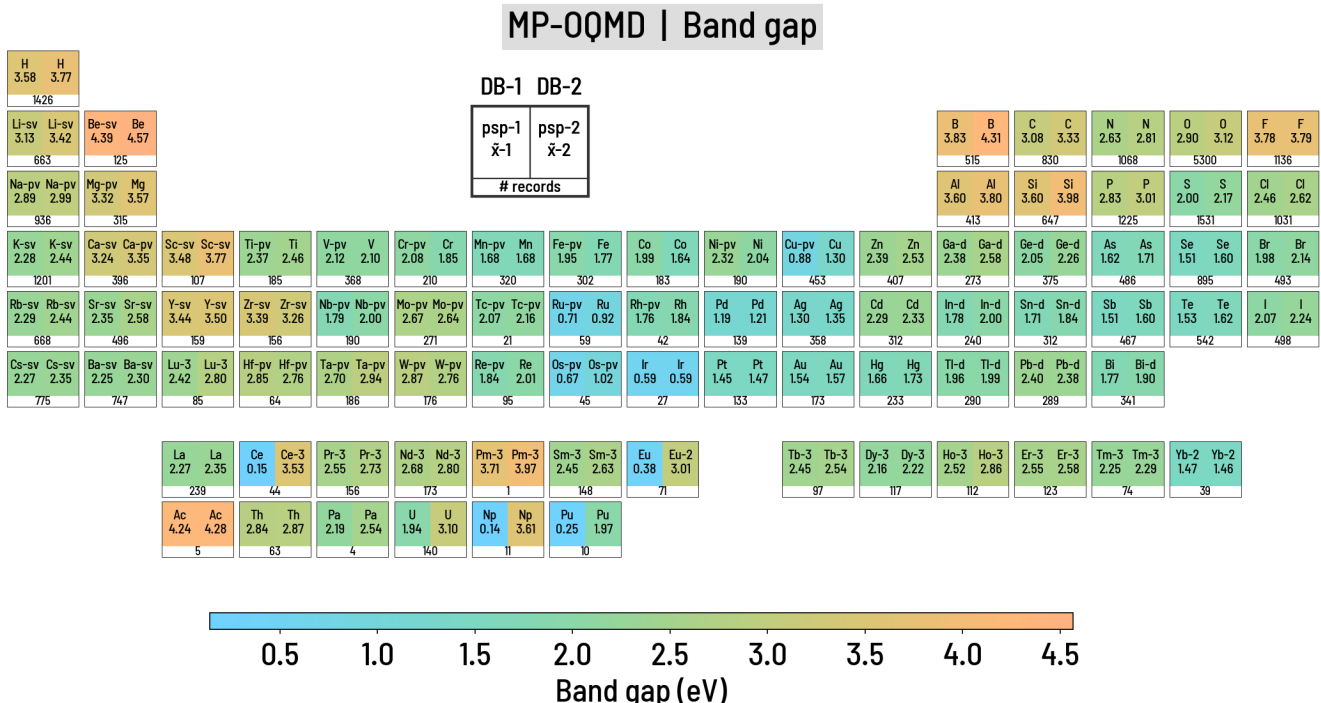


FIG. S12. Median values of band gap for compounds containing a certain element in the periodic table, for a comparison of MP and OQMD. The VASP PAW potential used for each element and the number of records in each comparison are indicated (* indicates more than one pseudopotential used in the database overall for that element).

MP-OQMD | Total magnetization

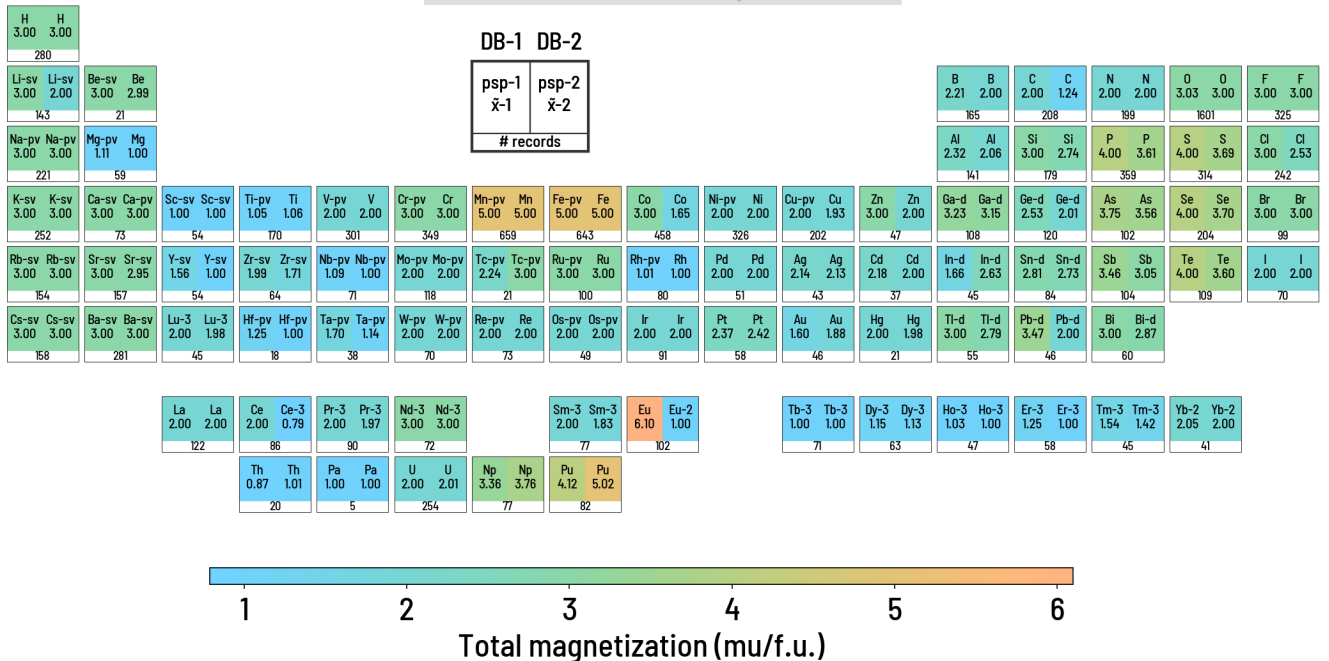


FIG. S13. Median values of total magnetization (per formula unit) for compounds containing a certain element in the periodic table, for a comparison of MP and OQMD. The VASP PAW potential used for each element and the number of records in each comparison (* indicates more than one pseudopotential used in the database overall for that element).

* These authors contributed equally to this work

† bryce@citrine.io

- ¹ S. Curtarolo, W. Setyawan, S. Wang, J. Xue, K. Yang, R. H. Taylor, L. J. Nelson, G. L. Hart, S. Sanvito, M. Buongiorno-Nardelli, *et al.*, *Comput. Mater. Sci.* **58**, 227 (2012).
- ² M. Widom and M. Mihalkovic, *J. Mater. Res.* **20**, 237 (2005).
- ³ J. S. Hummelshøj, F. Abild-Pedersen, F. Studt, T. Bligaard, and J. K. Nørskov, *Angew. Chem.* **124**, 278 (2012).
- ⁴ R. D. Johnson III, *NIST 101. Computational Chemistry Comparison and Benchmark Database*, Tech. Rep. (1999).
- ⁵ D. D. Landis, J. S. Hummelshøj, S. Nestorov, J. Greeley, M. Dułak, T. Bligaard, J. K. Nørskov, and K. W. Jacobsen, *Comput. Sci. Eng.* **14**, 51 (2012).
- ⁶ R. Tran, Z. Xu, D. W. Balachandran Radhakrishnan, W. Sun, K. A. Persson, and S. P. Ong, *Sci. Data* **3** (2016).
- ⁷ J. Hachmann, R. Olivares-Amaya, S. Atahan-Evrénk, C. Amador-Bedolla, R. S. Sánchez-Carrera, A. Gold-Parker, L. Vogt, A. M. Brockway, and A. Aspuru-Guzik, *J. Phys. Chem. Lett.* **2**, 2241 (2011).
- ⁸ K. Choudhary, I. Kalish, R. Beams, and F. Tavazza, *Sci. Rep.* **7** (2017).
- ⁹ V. Stevanović, S. Lany, X. Zhang, and A. Zunger, *Phys. Rev. B* **85**, 115104 (2012).
- ¹⁰ A. Jain, S. P. Ong, G. Hautier, W. Chen, W. D. Richards, S. Dacek, S. Cholia, D. Gunter, D. Skinner, G. Ceder, *et al.*, *APL Mater.* **1**, 011002 (2013).
- ¹¹ J. E. Saal, S. Kirklin, M. Aykol, B. Meredig, and C. Wolverton, *JOM* **65**, 1501 (2013).
- ¹² P. Gorai, D. Gao, B. Ortiz, S. Miller, S. A. Barnett, T. Mason, Q. Lv, V. Stevanović, and E. S. Toberer, *Comput. Mater. Sci.* **112**, 368 (2016).
- ¹³ W. Setyawan and S. Curtarolo, *Comput. Mater. Sci.* **49**, 299 (2010).
- ¹⁴ G. Pizzi, A. Cepellotti, R. Sabatini, N. Marzari, and B. Kozinsky, *Comput. Mater. Sci.* **111**, 218 (2016).
- ¹⁵ A. Larsen, J. Mortensen, J. Blomqvist, I. Castelli, R. Christensen, M. Dulak, J. Friis, M. Groves, B. Hammer, C. Hargus, *et al.*, *J. Phys. Condens. Matter* **29**, 273002 (2017).
- ¹⁶ K. Mathew, A. K. Singh, J. J. Gabriel, K. Choudhary, S. B. Sinnott, A. V. Davydov, F. Tavazza, and R. G. Hennig, *Comput. Mater. Sci.* **122**, 183 (2016).
- ¹⁷ S. P. Ong, W. D. Richards, A. Jain, G. Hautier, M. Kocher, S. Cholia, D. Gunter, V. L. Chevrier, K. A. Persson, and G. Ceder, *Comput. Mater. Sci.* **68**, 314 (2013).
- ¹⁸ S. Kirklin, J. E. Saal, B. Meredig, A. Thompson, J. W. Doak, M. Aykol, S. Rühl, and C. Wolverton, *npj Comput. Mater.* **1**, 15010 (2015).
- ¹⁹ A. Khorshidi and A. A. Peterson, *Comput. Phys. Commun.* **207**, 310 (2016).
- ²⁰ A. Van De Walle, M. Asta, and G. Ceder, *Calphad* **26**, 539 (2002).
- ²¹ K. Mathew, J. H. Montoya, A. Faghaninia, S. Dwarakanath, M. Aykol, H. Tang, I.-h. Chu, T. Smidt, B. Bocklund, M. Horton, *et al.*, *Comput. Mater. Sci.* **139**, 140 (2017).
- ²² Y. Wang, J. Lv, L. Zhu, and Y. Ma, *Comput. Phys. Commun.* **183**, 2063 (2012).
- ²³ T. Mayeshiba, H. Wu, T. Angsten, A. Kaczmarowski, Z. Song, G. Jenness, W. Xie, and D. Morgan, *Comput. Mater. Sci.* **126**, 90 (2017).
- ²⁴ A. Togo and I. Tanaka, *Scr. Mater.* **108**, 1 (2015).
- ²⁵ Y. Hinuma, G. Pizzi, Y. Kumagai, F. Oba, and I. Tanaka, *Comput. Mater. Sci.* **128**, 140 (2017).
- ²⁶ Q.-J. Hong and A. van de Walle, *Calphad* **52**, 88 (2016).
- ²⁷ C. W. Glass, A. R. Oganov, and N. Hansen, *Comput. Phys. Commun.* **175**, 713 (2006).
- ²⁸ D. C. Lonie and E. Zurek, *Comput. Phys. Commun.* **182**, 372 (2011).
- ²⁹ J. O'Mara, B. Meredig, and K. Michel, *JOM* **68**, 2031 (2016).
- ³⁰ K. Michel and B. Meredig, *MRS Bull.* **41**, 617 (2016).
- ³¹ “pypif: Python toolkit for working with PIFs,” <https://github.com/CitrineInformatics/pypif> (2018), accessed: May 2020.
- ³² S. P. Ong, S. Cholia, A. Jain, M. Brafman, D. Gunter, G. Ceder, and K. A. Persson, *Comput. Mater. Sci.* **97**, 209 (2015).
- ³³ C. Toher, Private communication (2018).
- ³⁴ “The Materials Project: The Materials API,” <https://materialsproject.org/docs/api>, accessed: December 2019.